A mutation of a single core gene, *tssM*, of Type VI secretion system of *Xanthomonas perforans* influences virulence, epiphytic survival and transmission during pathogenesis on tomato

Prabha Liyanapathiranage[a], Jeffrey B Jones[b] and Neha Potnis[a]

[a]Department of Entomology and Plant Pathology, Auburn University, Auburn, AL 36849, USA

[b]Department of Plant Pathology, University of Florida, Gainesville, FL 32611, USA

Corresponding Author: Neha Potnis nzp0024@auburn.edu

Abstract

Xanthomonas perforans is a seed-borne hemi-biotrophic pathogen that successfully establishes infection in the phyllosphere of tomato. While the majority of the studies investigating mechanistic basis of pathogenesis have focused on successful apoplastic growth, factors important during asymptomatic colonization in the early stages of disease development are not well understood. In this study, we show that *tssM* gene of the type VI secretion system cluster i3* (T6SS-i3*) plays a significant role during initial asymptomatic epiphytic colonization at different stages during the life cycle of the pathogen. Mutation in a core gene, *tssM* of T6SS-i3*, imparted higher aggressiveness to the pathogen, as indicated by higher overall disease severity, higher in planta growth as well as shorter latent infection period compared to the wild-type upon dip-inoculation of 4-5-week-old tomato plants. Contribution of *tssM* towards aggressiveness was evident during vertical transmission from seed-to-seedling with wild-type showing reduced disease severity as well as lower in planta populations on seedlings compared to the mutant. Presence of functional TssM offered higher epiphytic fitness as well as higher dissemination potential to the pathogen when tested in an experimental setup mimicking transplant house

high-humidity conditions. We showed higher osmotolerance being one mechanism by which TssM offers higher epiphytic fitness. Taken together, these data reveal that functional TssM plays a larger role in offering ecological advantage to the pathogen. TssM prolongs the association of hemi-biotrophic pathogen with the host, minimizing overall disease severity, yet facilitating successful dissemination.

Key Words: T6SS, *tssM*, latent infection, epiphytic, *Xanthomonas perforans*

Introduction

Successful infection by bacterial plant pathogens is a result of a complex, multifaceted process mediated by multiple pathogenicity determinants that function across different stages of the infection, asymptomatic, pathogenic and dissemination phase. In case of foliar plant pathogens, adaptation to the phyllosphere environment and successful niche occupancy is a crucial phase during which pathogen successfully overcomes nutritional limitation, water limitation, host defense, competition with the resident microflora and the environmental stress. This phase is followed by pathogenic phase that involves successful apoplastic colonization, suppression of host defense and extensive multiplication. Being equipped with the secretion systems that can facilitate the translocation of bacterial effectors outside of the cell membrane into the extracellular environment or directly into the host cell, allow phytopathogenic bacteria to establish successful infection. To date, 10 different secretion systems (systems I - X) have been identified in Gram-negative bacteria (Buttner and Bonas, 2010, Palmer et al. 2020; Meuskens et al. 2019) . While these secretion systems have been largely characterized for their importance

during pathogenic phase, their role during initial asymptomatic colonization is an unexplored area. Recent studies with *Pseudomonas syringae* have revealed genetic determinants that allow successful adaptation to epiphytic vs apoplastic lifestyle of the pathogen. These determinants include genes involved in flagellar, swarming motility, chemosensing, chemotaxis, osmotolerance, phenylalanine degradation being important for epiphytic colonization and can explain the response of a foliar pathogen to conditions experienced as an epiphyte (Helmann et al. 2019).

During *in planta* screening of the mariner transposon mutant library of *X. perforans* strain 91-118 (also referred to as *X. euvesicatoria* pv. *perforans* (Barak et al. 2016)) by dip-inoculation of tomato, we identified transposon mutant disrupting *tssM* gene of type VI secretion system cluster i3* (T6SS-i3*) that displayed more aggressive symptoms as well as quicker symptom development when compared to the disease progression by wild type strain. This observation led us to hypothesize that *tssM* gene of T6SS-i3* cluster plays a role during the asymptomatic phase. T6SS was initially described as nodulation impairment locus (imp) in *Rhizobium leguminosarum* and later identified and characterized in *Vibrio cholerae* (Pukatzki et al. 2006) and *Pseudomonas aeruginosa* (Mougous 2006). The genes encoding T6SS are distributed in approximately 25% of the sequenced gram-negative bacteria, mainly in the phylum Proteobacteria including pathogenic, beneficial and commensal bacteria (Boyer et al. 2009; Durand et al. 2014). Among the bacterial species that have T6SS encoded in their genome, many may contain 1-6 copies of complete T6SS clusters and many more copies of incomplete clusters of individual genes (Boyer et al. 2009). In the genus *Xanthomonas* two types of T6 clusters have been described as i3* and i3***, based on phylogenetic subclades within clade i3 based on *tssC*

gene (Bayer-Santos et al. 2019). T6SS cluster assembles from 13 core components, where at least 11 are structural proteins and two structural/ effector proteins (Hcp and VgrG) (Bingle et al. 2008). A subset of these core genes have evolutionary similarities to T4SS components or to bacteriophage and the whole system of T6SS shows structural and functional similarities to contractile bacteriophage cell puncturing device (Boyer et al. 2009; Cascales and Cambillau 2012). This contact-dependent nanomachinery can directly deliver secreted effectors or toxins into diverse neighboring cellular targets including both prokaryotic and eukaryotic organisms (Alcoforado Diniz et al. 2015). Each of these core components are essential for function, and inactivation of any of these 13 core components leads to significant defects in secretion.

IcmF family TssM is one of the conserved proteins involved in the assembly of inner membrane-spanning complex of the T6SS, that forms a hollow space to allow inner tube and effectors to travel through. In *Agrobacterium tumefaciens*, TssM has ATP binding and hydrolysis ability to enable the secretion of known T6 effector hemolysin-coregulated protein (Hcp) (Zoued et al. 2014; Ma et al. 2012). The electron microscopy of this inner membrane complex composed of TssJ, TssL and the important connector protein, TssM, in *E. coli* revealed that trans-envelope structure with double concentric ring like flexible structure containing 10 TssM and 10 TssJ proteins bound to each other and with arches containing 10 TssL copies (Durand et al. 2015) TssM, being a connector of inner membrane and outer membrane, can explain how the mutation of the TssM (Type six secretion core gene M) inner membrane protein, aborts the secretion of the effector protein Hcp (hemolysin-coregulated protein) (Chow and Mazmanian 2010; Mattinen et al. 2008; Weber et al. 2013; Wang et al. 2021), hence indicating the importance of the uninterrupted core genes for the secretion of the type 6 effectors.

The role of T6SS appears to be varying depending on the bacterial species, host species and host tissue also the distribution of the T6SS among the commensal as well as phytopathogenic bacteria suggests that the role of T6SS is beyond virulence (Bernal et al. 2018). While known primarily for mediating competition with prokaryotes or unicellular eukaryotes (Ma et al. 2014, Bernal et al. 2018, Bayer-Santos et al. 2018), T6SS has been shown to be important in virulence (Ge et al. 2008; Weber et al. 2013; Shalom et al. 2007), host colonization (Pezoa et al. 2014; de Pace et al. 2011) and intracellular multiplication (Chow and Mazmanian 2010; Parsons and Heffron 2005). In case of plant pathogenic bacteria, mutation of T6SS core gene has been associated primarily with impaired virulence as seen with *Agrobacterium tumefaciens* (Wu et al. 2008), *Pseudomonas syringae* pv. actinidiae*, Ralstonia solanacearum, Erwinia amylovora, Xanthomonas oryzae* pv. oryzae, *Xanthomonas phaseoli* pv manihotis, and *Burkholderia glumae BGR1* (Zhang et al. 2012; Tian et al. 2017; Wang et al. 2021; Choi et al. 2020; Montenegro Benavides et al. 2021, Kim et al. 2020).

While above examples illustrate inactivation of core genes of T6SS resulting in decreased virulence, our preliminary findings of increased aggressiveness associated with inactivation of *tssM* of T6SS-i3 cluster were contrasting. In this study, we investigated the contribution of TssM towards overall pathogenesis of bacterial leaf spot *Xanthomonas*. We examined crucial points of the bacterial leaf spot *Xanthomonas* life cycle, seed-to-seedling, seedlings at the transplant houses and leaf surfaces of mature plants, which are often control points for disease management. However, these are also control points at which failure of current management practices is noted, likely due to ability of pathogen to maintain asymptomatic colonization. Our findings demonstrate that functional TssM contributes towards early events of asymptomatic

colonization and adaptation in response to epiphytic stress. Delayed symptom development allows hemi-biotrophic *X. perforans* to prolong its association with the host while minimizing overall disease severity.

Experimental procedure

Bacterial strains, media and growth conditions

Bacterial strains and plasmids used in this study are listed in Table 1. *Xanthomonas perforans* was grown for 24h at 28^{o}C on Nutrient agar (NA) (Difco) and *E.coli* was cultivated in Luria-Bertani (LB) agar or broth at 37^{o}C (Miller 1972). When required antibiotics were added into the media to maintain selection for resistance markers at following working concentration: kanamycin (Km), 50µg/ml; nalidixic (Nal), 50 µg/ml; streptomycin (Strep), 50 µg/ml; rifampicin (Rif), 50 µg/ml, spectinomycin (Spec) 100 µg/ml, tetracycline (Tet) 12.5 µg/ml. All the strains were stored in sterile tap water at room temperature or in 30% glycerol at -80^{o}C or both. Triparental matings were performed on nutrient yeast extract glycerol agar (NYGA) (Turner et al. 1984).

Plant material and growth conditions

Tomato cultivar FL8000 was used in this study. Two-week-old seedlings were transplanted into sterile 4" plastic pots (The HC Companies, OH, USA) with soil-less potting medium (Premier Tech Horticulture, PA, USA). Plants were kept under 16h light per day at 28-30^{0}C under greenhouse conditions up to 4-5 weeks.

Construction of the in-frame deletion mutant AL65Δ*tssM*

X. perforans AL65 strain, isolated from symptomatic pepper plants in Alabama in 2017, was chosen to construct a null mutant since this strain was pathogenic on both tomato and pepper (Newberry et al. 2019), in addition to this strain being recently isolated and comparatively aggressive in relation to other *X. perforans* strains such as *Xp*91-118 (data not shown). A 900 bp promoter fragment upstream of the *tssM* (locus tag E2P69_09425, GenBank TVS54510.1) ORF (up)(tssMupF-TTGCAGGCGCGTTTGAAC, tssMupR-CTTGCGTAGCAACTGGATCG) and 852bp fragment downstream of the *tssM* ORF (down) (tssMdownF- ATATCGAAGGCCAGCGCTA, tssMdownR- AGATACATCTGGGCGGTGG) were PCR amplified using Phusion high-fidelity DNA polymerase (Thermo Scientific) according to the manufacturer's instructions. Both of these fragments were individually cloned into pCR™8/GW/TOPO® (Invitrogen) vector with *attL1*/ *attL2* sites. Primer sets, M13F/SR (M13F- GTAAAACGACGGCCAG, SR-CGTGCGCCGGCATGCCGTCATTCCCCAGGC) and SF/M13R (SF-GCCTGGGGAATGACGGCATGCCGGCGCACG, M13R- CAGGAAACAGCTATGAC) were used to amplify the upstream and downstream fragments in parallel with the short overlapping ends. Gel purified PCR fragments from the previous parallel reactions were fused together through a single overlap extension PCR reaction. PCR cycling parameters were designed according to the Phusion DNA polymerase guidelines (User Guide: Phusion High-Fidelity DNA Polymerase). Resulting 1100 bp overlapping fragment, representing Δ*tssM* with flanking upstream and downstream regions and the *attL1*/*attL2* sites was cloned into pCR™-Blunt II-TOPO. Next, 1100 bp Δ*tssM* fragment in pCR™-Blunt II-TOPO was recombined into the suicide vector pLVC18-Rfc (obtained from Mudgett's Lab) by a Gateway LR reaction (Invitrogen) (Atanassov et al. 2009). pLVC18-RfC (Δ*tssM*) was moved into AL65 by triparental mating, using *E. coli* helper strain containing pRK2073

plasmid. Single crossover events were selected by growth on NYGA media containing Rif and Tet antibiotics. SacB counter-selectable marker was used to select for a second crossover event by plating previously selected colonies on NYGA media containing 5% sucrose. Several subcultures were conducted to identify the deletion mutants generated through homologous recombination. Strains were selected for growth on NA containing Rif and for loss of growth on NA containing Tet (12.5 ug/ml). A deletion mutant AL65Δ*tssM* was confirmed by PCR using gene specific primers followed by sequence analysis as well as using whole genome sequencing followed by sequence analysis. The genome sequence of the deletion mutant was compared with the wild-type AL65 genome sequence to confirm in-frame non-polar deletion mutation of *tssM* gene of T6SS-i3 cluster.

Construction of AL65Δ*tssM* complement

Genomic region containing *tssM* promoter (900 bp upstream of the ORF), the *tssM* ORF (4593 bp) and 852 bp downstream of the ORF was PCR amplified from *Xp*AL65 using tssMupF and tssMdownR primers. This DNA fragment (6345 bp) was cloned into pENTR/D-TOPO vector and was recombined into the expression vector pDSK519 by a Gateway LR reaction (Invitrogen) (Atanassov et al. 2009). The resulting construct pDSK519 (*tssM*) was introduced into the AL65Δ*tssM* mutant by electroporation (1.8kV/4ms). Complement (AL65Δ*tssM*(*tssM*)) was confirmed by PCR, DNA sequencing and whole-genome sequencing.

***In planta* population study – dip inoculation using individual strains and mixed inoculum**

To determine the effect of *tssM* mutation on overall disease development by *X. perforans* pathogenicity, 4-5-week-old tomato cv. FL8000 plants were dip inoculated (30s) in a 600 ml cell

suspensions containing ~1 X 10^6 cfu/ml of *X. perforans* AL65^{strep}/ AL65Δ*tssM*^{nal}/ AL65Δ*tssM*(*tssM*)^{km} alone or AL65^{strep} + AL65Δ*tssM*^{nal} / AL65Δ*tssM*^{nal} + AL65Δ*tssM*(*tssM*)^{km} mixed in 1: 1 ratio for the mix inoculation study. Inoculum suspensions were amended with 0.0025% (vol/vol) Silwet 77. Both individual and mixed inoculations were conducted simultaneously so the overall disease severity levels can be compared in individual vs mixed inoculations. Plants dipped in sterile 0.01M $MgSO_4$ amended with 0.0025% (vol/vol) Silwet 77 were used as mock inoculations. The initial inocula were plated onto NA amended with antibiotics to confirm a 1:1 ratio of wild-type and mutant concentrations and complement and mutant concentrations. Inoculated plants were placed inside closed boxes and kept in a growth chamber at 25^{o}C with 12h light/dark cycle for 2 days after inoculation to facilitate high humidity. After the initial 48 h plants were maintained at high humidity for 12 hours in the dark and at low humidity for 12 hours in light. Middle leaflet samples were taken at every alternate day for 14 days and *in planta* bacterial populations were determined. At each sampling point, ~ 3 cm^2 area of leaflet tissues were taken from each plant using a sterile cork borer. Using sterile forceps leaf discs were placed inside sterile microcentrifuge tubes containing 1 ml sterile 0.01M $MgSO_4$ buffer and macerated using a sterile homogenizer. Ten-fold serial dilutions of the homogenized suspension were plated on antibiotic amended plates using spiral plater (Neu-tec Group Inc, NY, USA) to estimate the population size of AL65, AL65*ΔtssM*, and AL65Δ*tssM*(*tssM*) in individual inoculations and mixed inoculations. Plates were kept at 28^{o}C for 3 days before quantifying the colony counts. Bacterial populations were determined as colony forming units (cfu) per cm^2 of leaf area. Bacterial spot severity was recorded using the following scale and mean disease severity was calculated.

Disease scale: 1 = symptomless, 2 = a few necrotic spots on a few leaflets, 3 = a few necrotic spots on many leaflets, 4 = many spots with coalescence on few leaflets, 5 = many spots with coalescence on many leaflets, 6= severe disease and leaf defoliation, and 7= plant dead (Abbasi et al. 2002). This experiment was repeated three times and each treatment consisted of three replicates and results of a single representative experiment is shown the results section.

Plots of $\log_{10}$ cfu/cm^2 against time were generated and used to calculate the area under the growth progress curve (AUGPC) using the following formula.

$$\mathrm{AUGPC} = \sum_{i=1}[[(Y_{i+n1} + Y_i)/2)\ (X_{i+1} - X_i)]$$

Y_i = bacterial population at the ith observation, X_i = time in hours at the ith observation, and n = the total number of observations (Dutta et al. 2014a, 2014b).

In planta population study – infiltration inoculation

Four-to-five-week-old Tomato cv. FL8000 plants were inoculated with cell suspensions containing ~1 X 10^5 cfu/ml of *X. perforans* AL65^{strep}/ AL65Δ*tssM*^{nal}/ AL65Δ*tssM*(*tssM*)^{km} using a needleless syringe. Plants infiltrated with sterile 0.01M $MgSO_4$ were used as mock inoculations. Inoculated plants were kept in a growth chamber at 25^{o}C with 12h light/dark cycle for 8 days after inoculation. Middle leaflet samples were taken at every alternate day for 8 days and *in planta* bacterial populations were determined as described in the previous section. This experiment was repeated two times and each treatment consisted of three replicates and results of a single representative experiment is shown the results section.

Determination of epiphytic and total populations of *X. perforans* under high-humidity transplant house-mimic conditions

Humidity chambers were constructed in the greenhouse to mimic conditions inside a seedling transplant house that facilitates conditions conductive for BLS disease development. Each humidity chamber frame was built with PVC pipes and covered with transparent polythene sheets from all sides. Inside each chamber, high relative humidity was maintained by using a sprinkler irrigation system providing overhead irrigation (set to water at 0800 and 1800h for 1 minute on each occasion each day). Six 128-cell trays with two-week-old seedlings were arranged inside a single chamber. Plants were fertigated two weeks after sowing and every week after that until the end of the trial. To investigate the role of TssM on epiphytic survival and dissemination, two-week-old tomato cv FL8000 seedlings from the first row of the trays were inoculated with a 1: 1 mixed inoculum of AL65^{step} and AL65Δ*tssM*^{nal} or AL65Δ*tssM*^{nal} and AL65Δ*tssM*(*tssM*)^{km} at 10^6 CFU/ml concentration. Inoculum suspensions were amended with 0.0025% (vol/vol) Silwet 77. The leaflets were sampled at 9 sampling points for estimating epiphytic and total population of wild-type, mutant and complement on day 7, 14 and 21 post-inoculation. For estimating epiphytic population, leaves were placed in a ziplock bag, weighed, and then suspended in phosphate-buffered saline solution (50mM) amended with 0.02% Tween 20 followed by sonication for 10 minutes. The leaf washings were serially diluted and plated on antibiotic amended media using spiral plater (Neu-tec Group Inc, NY, USA) and bacterial populations were estimated as $\log_{10}$ cfu/g of leaf tissue. For estimating total population, sampled leaflets were macerated and the homogenate was plated upon serial dilutions on antibiotic amended media. At each sampling point, at each sampling time, the number of tomato seedling that showed BLS

symptoms were recorded to calculate proportion infected/symptomless to correlate that to the population of each strain found in different sampling points (Dutta et al. 2014a). Plots of $\log_{10}$ cfu/g against time were generated and used to calculate the area under the growth progress curve (AUGPC) (Dutta et al. 2014a, 2014b). The experiment was repeated at least three times with two replicates in each treatment and results of a single representative experiment is shown the results section.

Seed-to-seedling disease transmission assay

To determine the influence of inactivation of TssM on seed-to-seedling disease transmission, Tomato cv. FL8000 seeds were inoculated by immersion in individual cell suspensions containing ~1 X 10^6 cfu/ml of antibiotic-marked strains of *X. perforans* AL65^{step}, AL65Δ*tssM*^{nal} and AL65Δ*tssM*(*tssM*)^{km} for 2 hours. Seeds treated with double-distilled water were used as mock inoculations. Inoculated seeds were then air-dried at room temperature for 24 hours as described previously (Tian et al. 2015). Sterile plastic pots (The HC Companies, OH, USA) with soil-less potting medium (Premier Tech Horticulture, PA, USA) were used to place 3 seeds from each treatment and it served as a single biological replication. Twenty-one day old seedlings were evaluated for BLS severity at the end of the trials based on disease index, as described previously (Tian et al. 2015). The disease severity scale ranged from '0 – 5'; '0'- no symptoms: '1' water-soaked lesions on approximately 25% of the cotyledons: '2'- water-soaked lesions on approximately 50% of the cotyledons: '3', water-soaked lesions on approximately 75% of the cotyledons: '4', water-soaked lesions spread on 100% of the cotyledons: and '5', total death of the seedling. The disease index (DI) was calculated at the end of the trial based on the following

formula, where A is the previously described disease scales and B is the number of plants with water-soaked lesion percentages described in that disease scale per treatment.

$$\mathrm{DI} = \sum(\mathrm{A\ X\ B})\mathrm{X}100/\sum \mathrm{BX}5$$

Bacterial populations on germinating tomato seedlings were determined by macerating leaves of 21 days old seedlings followed by appropriate serial dilutions of each homogenate replicate on NA plates amended with appropriate antibiotics using spiral plater (Neu-tec Group Inc, NY, USA) and incubated for 2-3 days at 28^{o}C. Colonies were counted and colony-forming units cfu per gram of plant tissue were calculated. This experiment was repeated three times and each treatment consisted of three replicates and results of a single representative experiment is shown the results section.

Growth of the bacterial strains under in-vitro conditions

In-vitro growth assay was conducted to evaluate if there is any growth defect in the AL65Δ*tssM* strain due to the mutation. AL65^{step}, AL65Δ*tssM*^{nal} and AL65Δ*tssM*(*tssM*)^{km} were grown for 24h on NA media amended with respective antibiotics. Bacterial growth was suspended on XVM2: hrp-inducing minimal medium (Wengelnik et al. 1996) and grew for 24 hours. Bacterial growth was collected by centrifugation and washed twice by XVM2 medium and subcultured twice in the same minimal medium. When the cells reached the late-log phase (0.27-0.3 OD_{600} = 10^8 cfu/ml), they were collected by the centrifugation at 5000 X g for 10 minutes. The cell pellets were resuspended in the XVM2 to a final concentration of 10^8 cfu/ml. Aliquots were transferred to microcentrifuge tubes and diluted to 5X10^4 cfu/ml with XVM2. Two hundred microliters of the

suspensions were placed on 96 well plate at 28^{o}C at 140rpm and OD_{600} was measured every 12 hours.

Since our observations with previous experiments were showing a role of TssM in epiphytic survival of *Xanthomonas perforans,* we wanted to further test if TssM has any other functions in successful survival in the leaf surface. As water availability is one of the barriers faced by the leaf pathogens, in-vitro osmotolerance assay was conducted. To conduct this assay, bacterial strains grown in corresponding antibiotics amended media were suspended on XVM2 media and grew for 24 hours. Bacterial cell pellets collected after the centrifugation were washed twice with XVM2 medium and subcultured in the same minimal medium. This step was repeated one more time. When the cells reached the late-log phase (0.27-0.3 OD_{600} = 10^8 cfu/ml), they were collected by the centrifugation at 5000 X g for 10 minutes and suspended in the medium lacking NaCl to a final concentration of 10^8 cfu/ml. Aliquots were transferred to microcentrifuge tubes and diluted to $5X10^4$ cfu/ml with XVM2 with different NaCl concentrations (0M -1M). Two hundred microliters of the suspensions were placed on 96 well plates at 28^{o}C at 140rpm and OD_{600} was measured every 12 hours. To further confirm the viable cell count during the bacterial growth at different NaCl concentrations, experiments was repeated and at sampling points 0h, 30h and 60h, 10 µl of each bacterial suspension was taken and plated on NA media amended with corresponding antibiotics for appropriate dilutions. In-vitro growth assay and In-vitro osmotolerance assays were repeated three times and each treatment consisted of three replicates and results of a single representative experiment are shown the results section.

Results

Mutation in the *Xanthomonas perforans* T6SS-i3* core gene, *tssM*, results in increased virulence

In this study, we constructed an in-frame deletion mutant of *tssM* (a null mutant, referred to as, AL65Δ*tssM*, hereafter) and a complement by extrachromosomal expression of TssM under the control of a native promoter (referred to as, AL65Δ*tssM(tssM)*, hereafter). The resultant deletion mutant was subjected to whole genome re-sequencing. Deletion of the open-reading frame of *tssM* confirmed the non-polarity of the mutation. Virulence potential of these constructs was evaluated by dip-inoculating susceptible FL8000 tomato leaves of 4-5-week-old plants with a bacterial suspension adjusted to 10^6 CFU/ml consisting of wild-type (AL65), or a 1:1 ratio of AL65Δ*tssM* or AL65Δ*tssM(tssM),* by monitoring growth of these strains and symptom development *in planta* over two weeks. AL65Δ*tssM* mutant exhibited quicker disease symptom development, as early as 3 dpi whereas AL65 and AL65Δ*tssM(tssM)* strains showed watersoaking lesions by 4 dpi (Figure 1). This delayed symptom development with the AL65 and AL65Δ*tssM(tssM)* strains also directly correlated with the lower titers starting at 4 dpi through 14 dpi. Population of the AL65Δ*tssM* started to increase rapidly after 2 dpi and maintained ~0.5 to 1 $\log_{10}$ higher population compared to the AL65 and AL65Δ*tssM(tssM)* strains throughout the course of the experiment (Figure 2a). These observations on overall symptom development as well as in planta growth with AL65Δ*tssM* were similar to that of our initial observations with the transposon mutation in *tssM* gene identified in *Xp*91-118 background (data not shown), confirming the similar phenotype of mutation in different strain background. Next, we compared growth progress curves of these strains. AUGPC value for AL65Δ*tssM* was significantly higher than those for AL65 and AL65Δ*tssM*(*tssM*) strains ($p<0.05$). There was no significant difference in

AUGPC between wild-type and AL65*ΔtssM*(*tssM*) strains (Figure 2a) or in the bacterial growth at any sampling day. AL65*ΔtssM* inoculated leaves had higher disease severity compared to leaves inoculated with AL65 or AL65Δ*tssM(tssM)* strains (Figure 3a &c). Overall, AL65*ΔtssM* was more aggressive on tomato compared to the wild-type and had a comparatively shorter latent period compared to the wild-type.

Mixed infection does not provide a competitive advantage for the mutant over wild-type, but rather leads to reduced disease severity

Since the mutation in the *tssM* gene resulted in higher in planta population along with increased aggressiveness of the pathogen on tomato plants, we hypothesized that AL65*ΔtssM* will outcompete the wild type or complement during mixed infection of tomato plants with 1:1 ratio of either AL65 + AL65*ΔtssM* or AL65*ΔtssM(tssM) +* AL65*ΔtssM*. Mixed infection did not show significant differences in the AUGPC values of each strain, although the mutant grew to a slightly higher population in planta in few sampling points compared to wild-type and complement (Figure 2b & c) without any statistically significant difference. The most notable observation with mixed infection was lower disease severity in mixed infection compared to individual infections (Figure 3b &c).

Mutation in *tssM* does not contribute to the virulence of the pathogen when directly infiltrated into the apoplast

In the previous experiment we observed that mutation of *tssM* led to increased overall pathogen aggressiveness when the dip inoculation method was used and the pathogen was given a chance to establish epiphytic colonization, as it is seen under natural infection conditions. To test

whether deletion of *tssM* also influenced disease development during endophytic colonization of the pathogen, we performed an infiltration inoculation assay to artificially introduce AL65, AL65Δ*tssM* and AL65Δ*tssM(tssM)* strains directly into the apoplast. Water-soaking of lesions was observed by 3 dpi for all three treatments and the degree of severity was uniform among the strains. No significant differences were observed among three treatments at any sampling timepoint for bacterial titers (Figure 4a) as well as AUGPC (Figure 4b). No difference was observed in symptom development throughout the course of the experiment between AL65 and AL65Δ*tssM* (Figure 4c).

AL65Δ*tssM* displays lower epiphytic survival and reduced transmission compared to the wild-type.

Tomato seedlings are usually mass-produced inside high humidity transplant houses prior to their distribution to use in field transplanting. We tested contribution of functional TssM towards asymptomatic epiphytic colonization on tomato in transplant house-mimic conditions by enumerating the total (epiphytic and endophytic) population and epiphytic population weekly for up to 28 days. Total and epiphytic population counts for AL65, AL65*ΔtssM* and AL65*ΔtssM(tssM)* in each chamber at 7, 14 and 21 can be found in supplementary figures S1, S2 and S3 respectively). AUGPC values calculated based on weekly enumeration of epiphytic and total populations of AL65, AL65*ΔtssM(tssM)* and AL65*ΔtssM* up to 28 days revealed similar trends with higher values for AL65 and AL65*ΔtssM(tssM),* beyond sampling point 3 (Figure 5a &b). Although total population at the point of inoculation (sampling point 1) and the sampling point 2 was more than 1 log higher for AL65*ΔtssM* compared to the AL65 strain, we observed higher total

population of AL65 beyond 3rd sampling points at 28 dpi (Figure S4c). Similar observations were recorded with complement strain when AL65*ΔtssM*(*tssM*) and AL65*ΔtssM* were co-inoculated in a second humidity chamber (Figure S4b). Tomato seedlings were observed for disease symptoms at every 7, 14, 21 and 28 dpi and % of seedlings showing disease symptoms was calculated at each sampling point to understand the symptom development in each of the sampling point in relation to the bacterial population growth. Until 14 dpi BLS disease symptoms were only observed in sampling point 1 or 1 and 2 in both of the chambers and the infected seedling percentage was less than 30% in these two sampling points (Figure S5 a and b). There was absence of obvious symptoms at day 7 and 14 beyond sampling point 2 despite the presence of ~ 10^3 - 10^4 CFU/g epiphytic population on seedlings (Figure S1cd and S2cd). At 28dpi, more than 90% of the seedlings displayed disease symptoms in 1st and 2nd sampling points in both of the chambers with a gradual reduction in the disease incidence with <20% infection beyond sampling point 8 (1.7m) (Figure S5 a and b). Sampling point 9, the farthest sampling point from the inoculated plants, had <10% infection throughout the course of this experiment, yet supported significantly higher epiphytic (~0.5 log) populations for the wild type compared to the mutant at all sampling time points, indicating greater transmission potential of the wild type than mutant.

AL65Δ*tssM* is highly aggressive on seedlings eliciting more severe symptoms with higher population compared to the wild-type upon vertical transmission from seed to seedling.

With the observations of the previous experiments, we were intrigued to study the role of functional TssM in other stages of the disease cycle of BLS caused by *Xanthomonas perforans.* Since this is a seedborne pathogen, seed to seedling disease transmission of *Xanthomonas*

perforans was evaluated after inoculation of tomato seeds with AL65Δ*tssM*, AL65 and AL65Δ*tssM*(*tssM*). AL65Δ*tssM* strain showed significantly higher mean population growth of ~ 3 X 10^9 cfu/g compared to the AL65 strain and AL65Δ*tssM*(*tssM*) strain that showed mean population of ~ 6 X 10^8cfu/g and ~1 X 10^8cfu/g, respectively, on 21-day-old tomato seedlings (Figure 6a). AL65Δ*tssM* showed significantly higher mean BLS disease severity index of 60%, compared to AL65 and AL65Δ*tssM*(*tssM*) showing 33.33% disease severity (Figure 6b).

***X. perforans* wild-type exhibited a higher osmotolerance compared to the AL65*ΔtssM*.**

Previous experiments indicated that presence of functional TssM accounted for higher epiphytic survival and higher transmission potential. Thus, we hypothesized that wild type carrying functional TssM can effectively overcome environmental stresses encountered during epiphytic colonization. Since osmotolerance is an important trait for epiphytic survival of the pathogen due to low water availability, we evaluated the tolerance of AL65 and AL65*ΔtssM* to the osmotic stress during growth in XVM2 with varying concentration of NaCl. AL65*ΔtssM* was able to grow as well as the wild-type and the complement in XVM2 medium that mimics apoplastic environment, indicating a lack of an inherent growth defect in the mutant (Figure 7a). But as NaCl concentration was gradually increased to 0.1M and 0.2M, AL65 exhibited a higher growth dynamic compared to the AL65*ΔtssM* (Figure 7b &c respectively). Growth pattern in other NaCl concentrations did not show any difference among the tested strains (data not shown).

Discussion

In this study, we discovered the role of TssM of T6SS-i3* during three epidemiologically important stages of the life cycle of the bacterial leaf spot pathogen, *Xanthomonas*, namely, during seed to

seedling transmission, during survival on transplants and during pathogenesis of 4-5 week old mature tomato plants. Our data suggest that functional TssM imparts epiphytic fitness to the *Xanthomonas* pathogen, thus, allowing successful asymptomatic colonization of the pathogen. Having equipped with the functional TssM also delays the onset of the disease symptoms and lowers the pathogen titer in the susceptible tomato leaves when compared to the mutant, thus, suggesting its possible contribution towards ecology of the pathogen.

TssM is a connector protein involved in the inner membrane-spanning complex of T6SS. Since mutation of this core component aborts the secretion of T6SS effector proteins (Chow and Mazmanian 2010; Mattinen et al. 2008; Weber et al. 2013; Wang et al. 2021), the phenotypes associated with AL65*ΔtssM* observed in this study are a result of non-functional type VI secretion system, T6SS-i3. However, we cannot rule out a broad versatile role of TssM independent of T6SS. It is possible that pleiotropic effects observed in this study could be a result of a complex regulatory network involving TssM and/or T6SS-i3. Presence of two T6SSs clusters in *Xanthomonas perforans*, hence two *tssM* genes, raise a question about functional redundancy and hence, possible trans-complementation in case of a deletion mutant of a core gene of single T6SS cluster. The two *tssM* genes from cluster i3* and i3*** share only 65% identity at nucleotide level and 45% at amino acid level. In many pathogens carrying multiple T6SS clusters, such sequence divergence reflected different functional profiles and differential regulation (Navarro-Garcia et al. 2019; Sha et al. 2013; Pezoa et al. 2014, Zhang et al. 2011), suggesting inability to successfully complement the phenotype by other T6SS cluster genes. Lack of functionally redundancy also meant that each T6SS cluster is specialized to perform a particular phenotype such as virulence, or bacterial competition, or interaction with eukaryotic cells (Zhu et al. 2020).

Given the presence of two T6SS clusters in the pathosystem studied here, further studies with single and double mutants with t*ssM* gene deletions in both clusters i3* and i3*** would be needed to study phenotype profiles and differential regulation of these multiplied systems.

One of the striking finding of this study was faster symptom development and increased disease severity accompanied by increased in planta growth associated with AL65Δ*tssM*. This contrasts with the typical virulence factors, mutations of which typically lead to reduced virulence or reduced disease severity. Our observations suggest that TssM might function to limit aggressiveness of the pathogen. Aggressiveness is measured by two traits, latent infection period and disease severity. In plant pathogens the time between host infection and pathogen sporulation/multiplication due to that infection is referred as the latent period, a crucial life history trait (Lannou 2012; Pariaud et al. 2009). In addition to aggressiveness, we also observed increased in planta growth with AL65Δ*tssM*. This is indicative of the role of TssM in determining threshold in planta populations during infection. Similar observation of limit on intracellular pathogen titers during colonization of mouse in presence of T6SS of intracellular animal pathogen *Helicobacter hepaticus* was thought to suggest role of T6SS in promoting a symbiotic relationship between *H. hepaticus* and mammals (Chow and Mazmanian 2010). Bacterial leaf spot pathogen, *Xanthomonas perforans*, is a hemibiotrophic pathogen that maintains colonization within host to promote its dissemination before inducing the host cell death. Such pathogenesis strategy might explain lower pathogen titers associated with functional TssM. We wondered if this lower titer might be due to higher cost associated with expressing TssM and hence T6SS. We ruled out a growth defect due to presence or absence of TssM under in vitro conditions, i.e. in minimal XVM2 medium, under which T6SS-i3* expression is observed. However, we cannot rule out inherent

differences in expression patterns observed under in vitro conditions and in planta conditions, and thus, cannot completely rule out the explanation of higher cost associated with expressing TssM in wild-type, leading to lower in planta titer when compared to *tssM* mutant. However, experiments involving mixed infection of wild type and *tssM* mutant and wild-type did not show effect on in planta population growth, yet lowered disease severity. This observation indicated that expression of TssM by wild-type influenced overall pathogen aggressiveness in the mixed infection, further confirming the contribution of TssM as a tolerance promoting factor by delaying disease symptom development and lowering pathogen titer.

We also observed the influence of the inoculation method on the AL65*ΔtssM* mutant phenotype. Infiltration i.e. artificial inoculation of the pathogen directly into the apoplast failed to show difference in overall pathogen titers or disease severity ratings between AL65 and the AL65Δ*tssM*. This observation coincided with the previous finding with mutants (deletion of *tssF, G* and *H* genes) in T6SS-i3* of *Xeu* where infiltration experiments in tomato/pepper concluded no role of T6SS in the pathogen virulence (Abendroth et al. 2017). In our experiment, since we used the dip-inoculation (mimicking natural infection) method we were able to identify the role of TssM in limiting virulence of pathogen and this emphasizes the importance of testing different methods of inoculation to test the contribution of genes/gene clusters towards pathogenesis.

Being a seed-borne pathogen, a critical control point considered in managing bacterial spot disease is seed-to-seedling transmission of the pathogen (Dutta et al. 2014a). While seed certification programs ensure supply of clean seeds to the growers, we continue to see bacterial spot outbreaks in the transplant houses and fields mainly originating from contaminated seeds,

especially with the seed lots with low contamination rates that might miss the seed testing protocols. Seedling-grow out assays are commonly used in seed certification programs (Gitaitis and Walcott 2007). Our findings of lower disease severity on seedlings infected with wild type compared to the AL65*ΔtssM* are suggestive of the contribution of TssM towards successful vertical transmission of pathogen from seed to seedling with little or no symptoms on seedlings. These observations are not in agreement with the evaluation of seed to seedling transmission of *Acidovorax citrulli xjl12* on melon seeds, where significant reduction in the disease index of melon seedlings inoculated with T6SS mutants *ΔvasD, ΔimpJ, ΔimpK* and *ΔimpF* was observed compared to wild-type, but no significant difference was observed in disease index with *impL* mutant (homologous to *tssM*) (Tian et al. 2015). These findings show a differential role of TssM in plant pathogenic bacteria. This could be possibly due to differential colonization strategies adopted by pathogens that require differential regulation and involvement of secretion systems during pathogenesis.

A functional TssM allowed successful transmission of the pathogen from seed to seedling with lower disease severity with lower in planta population compared to the *tssM* mutant. Despite low levels of disease severity and lower population levels on seedlings compared to the mutant, wild type with functional TssM was highly fit under high humidity transplant house mimic conditions. A functional TssM imparted higher epiphytic survival to the pathogen and allowed dissemination into the longer distances of ~2m as early as 7 days post-inoculation, with populations of ~10^4 CFU/g, despite <10% disease incidence. This asymptomatic spread of the pathogen to longer distances might allow pathogen to escape artificial selection in the transplant

houses, which are another epidemiologically important control point for managing bacterial spot disease (Abrahamian et al. 2019, Dutta et al. 2014a; Potnis et al. 2015)).

Given the importance of TssM associated phenotype at 3-4 days after dip-inoculation, we speculate that TssM functions at the early stages of *Xanthomonas* infection to allow successful adaptation of the pathogen to the phyllosphere during the asymptomatic phase. This is in line with the observation of activation of T6SS core genes including *tssM* as early as 3 h after inoculation of another hemi-biotrophic foliar pathogen *Pseudomonas syringae* pv. actinidiae on kiwifruit (McAtee et al. 2018). TssM alters the kinetics of the symptom development during bacterial spot pathogenesis. This may suggest involvement of TssM in direct or indirect regulation of virulence factors, mainly type III secretion system (T3SS) and associated effectors during early asymptomatic colonization. Ceseti et al. (2019) showed temporal induction patterns of T6SS and T3SS genes during pathogenesis of *Xanthomonas citri* pv. citri. They noted upregulation of the T6SS genes during the epiphytic growth of pathogen on citrus, with low expression levels of T6SS genes during apoplastic colonization. Type III secretion system genes and effectors were highly upregulated during colonization of the apoplastic space. A crosstalk between these two secretion systems during disease progression has been noted in several plant, animal, and human pathogens (Ceseti et al. 2019, Zhang et al. 2012, Wang et al. 2021, Moscoso et al. 2011, Records and Gross, 2010, Leung et al. 2011), with a complex regulatory network. Future work will be aimed at dissecting this regulatory network in hemibiotrophic pathogen during pathogenesis of tomato to understand the role of TssM in the overall kinetics of disease development.

Our findings of higher epiphytic survival of wild type compared to TssM mutant suggest a larger role of TssM towards ecology of this pathogen. Asymptomatic epiphytic survival of

512 the pathogen has been a major concern due to direct influence on effectiveness of management
513 strategies. Such epiphytic populations have been a culprit in reducing efficacy of bactericides as
514 well as impacting durability of disease resistance (Pernezny and Collins 1997). Phyllosphere is a
515 challenging environment influenced by biotic and abiotic factors. For a pathogen to successfully
516 establish in this environment, it must overcome these biotic and abiotic stresses encountered on
517 a leaf surface (Lindow and Brandl, 2003). One such stress is low water availability. Accumulation
518 of solutes on the leaf surface can lead to osmotic stress and thus, osmotolerance is an important
519 trait in bacteria that facilitate successful survival on the leaf surface. Presence of TssM in
520 *Xanthomonas* offers osmotic stress adaptation facilitating epiphytic colonization and growth of
521 the pathogen. Difference in the osmoadaptation mechanisms have proven to be influencing the
522 relative fitness of individual species and strains. For example, *P. syringae* B728a strain that shows
523 superior osmotolerance has shown to be better adapted for epiphytic survival than *P. syringae*
524 DC3000 and 1448A strains. A global transcriptomic analysis of *P. syringae* B728a and *P. syringae*
525 DC3000 strains performed under higher osmotic stress identified upregulation of T3SS and T6SS
526 genes in the *P. syringae* B728a (Freeman et al. 2013). Similar observations of upregulation of the
527 T6SS genes including *tssM* as a response to the salt-induced osmotic stress were recorded in
528 *Acidovorax avenae* subsp. *avenae RS-1* (Cui et al. 2015). Apart from osmotolerance, pathogen
529 has to overcome competition with the resident microbiome in order to establish itself. Higher
530 epiphytic fitness of the wild type with functional TssM might also suggest possible role of TssM
531 in mediating interactions with the resident microflora via T6SS. T6SS was first characterized in
532 *Pseudomonas aeruginosa* and *Vibrio cholerae* for its role in contact-dependent interbacterial
533 competition, where tit-for-tat type of interactions were noted (Basler et al. 2013). Such

534 counterattack mediated by T6SS and associated toxins against bacterial or eukaryotic
535 competitors were characterized in multiple animal, human and plant pathogenic bacteria (Russell
536 et al. 2011; MacIntyre et al. 2010; Song et al. 2021; Trunk et al. 2018; Storey et al. 2020,
537 Bayer-Santos et al. 2018, Zhu et al. 2020). Further studies investigating whether TssM-mediated
538 manipulation of resident microbiota results in altered host susceptibility would help disentangle
539 the functional profile of TssM not just in the context of virulence but in the context of its
540 ecological significance.
541 In conclusion, we present evidence for contribution of T6SS-i3* core gene *tssM* during some of
542 the crucial stages of the life cycle of the foliar hemi-biotrophic pathogen, seed-to-seedling
543 transmission, transplants and during asymptomatic colonization on mature 4-to-5-week-old
544 plants. Interestingly, in all these stages, TssM influences a crucial life history trait of latent
545 infection period. TssM dictates threshold in planta population, and thus, is determinant of
546 aggressiveness of the hemi-biotrophic foliar pathogen, *Xanthomonas.* We hypothesize that by
547 delaying the symptom development, TssM plays a role in prolonging association of the pathogen
548 with the host, thereby not only offering advantage in sustaining niche for the pathogen but also
549 ensuring successful dissemination. Given the fact that impact on latent infection period
550 influences the overall disease outcome, further studies focused on understanding the regulation
551 of pathogenesis by TssM during otherwise overlooked early asymptomatic colonization period
552 are crucial.
553
554 Acknowledgement

The authors thank Jane Farr and the Plant Science Center at Auburn University for providing the greenhouse resources necessary to conduct this work.

Funding: This work was funded by the USDA National Institute of Food and Agriculture, Hatch project 1012760, the Alabama Agricultural Experiment Station and NSF-CAREER award IOS – 1942956 to NP.

References

Abbasi, P. A., Soltani, N., Cuppels, D. A., and Lazarovits, G. 2002. Reduction of Bacterial Spot Disease Severity on Tomato and Pepper Plants with Foliar Applications of Ammonium Lignosulfonate and Potassium Phosphate. Plant Disease. 86:1232–1236.

Abendroth, U., Adlung, N., Otto, A., Grüneisen, B., Becher, D., and Bonas, U. 2017. Identification of new protein-coding genes with a potential role in the virulence of the plant pathogen Xanthomonas euvesicatoria. BMC Genomics. 18:625.

Abrahamian, P., Timilsina, S., Minsavage, G. V., Potnis, N., Jones, J. B., Goss, E. M., et al. 2019. Molecular Epidemiology of Xanthomonas perforans Outbreaks in Tomato Plants from Transplant to Field as Determined by Single-Nucleotide Polymorphism Analysis. Appl Environ Microbiol. 85.

Alcoforado Diniz, J., Liu, Y., and Coulthurst, S. J. 2015. Molecular weaponry: diverse effectors delivered by the Type VI secretion system. Cell Microbiol. 17:1742–1751.

Atanassov, I. I., Atanassov, I. I., Etchells, J. P., and Turner, S. R. 2009. A simple, flexible and efficient PCR-fusion/Gateway cloning procedure for gene fusion, site-directed mutagenesis, short sequence insertion and domain deletions and swaps. Plant Methods. 5:14.

Barak, J. D., Vancheva, T., Lefeuvre, P., Jones, J. B., Timilsina, S., Minsavage, G. V., Vallad, G. E., and Koebnik, R. 2016. Whole-Genome Sequences of Xanthomonas Euvesicatoria Strains Clarify Taxonomy and Reveal a Stepwise Erosion of Type 3 Effectors. Frontiers in Plant Science**.** 7, 1805.

Basler, M., Ho, B. T., and Mekalanos, J. J. 2013. Tit-for-Tat: Type VI Secretion System Counterattack during Bacterial Cell-Cell Interactions. Cell. 152:884–894.

Bayer-Santos, E., Ceseti, L. de M., Farah, C. S., and Alvarez-Martinez, C. E. 2019. Distribution, Function and Regulation of Type 6 Secretion Systems of Xanthomonadales. Front. Microbiol. 10:1635.

Bayer-Santos, E., Lima, L. dos P., Ceseti, L. de M., Ratagami, C. Y., Santana, E. S. de, Silva, A. M. da, et al. 2018. Xanthomonas citri T6SS mediates resistance to Dictyostelium predation and is regulated by an ECF σ factor and cognate Ser/Thr kinase. Environmental Microbiology. 20:1562–1575.

Bernal, P., Llamas, M. A., and Filloux, A. 2018. Type VI secretion systems in plant-associated bacteria. Environmental Microbiology. 20:1–15.

Bingle, L. E., Bailey, C. M., and Pallen, M. J. 2008. Type VI secretion: a beginner's guide. Current Opinion in Microbiology. 11:3–8.

Boyer, F., Fichant, G., Berthod, J., Vandenbrouck, Y., and Attree, I. 2009. Dissecting the bacterial type VI secretion system by a genome wide in silico analysis: what can be learned from available microbial genomic resources? BMC Genomics. 10:104.

Buttner, D., and Bonas, U. 2010. Regulation and secretion of Xanthomonas virulence factors. FEMS Microbiol. Rev. 34(2):107-33.

595 Cascales, E., and Cambillau, C. 2012. Structural biology of type VI secretion systems. Phil. Trans. R. Soc.
596 B. 367:1102–1111.
597 Ceseti, L. M., de Santana, E. S., Ratagami, C. Y., Barreiros, Y., Lima, L. D. P., Dunger, G., et al. 2019. The
598 Xanthomonas citri pv. citri Type VI Secretion System is Induced During Epiphytic Colonization of
599 Citrus. Curr Microbiol. 76:1105–1111.
600 Chen, L., Zou, Y., She, P., and Wu, Y. 2015. Composition, Function, and Regulation of T6SS in
601 Pseudomonas Aeruginosa. Microbiological Research. 172: 19–25.
602 Choi, Y., Kim, N., Mannaa, M., Kim, H., Park, J., Jung, H., et al. 2020. Characterization of Type VI Secretion
603 System in Xanthomonas oryzae pv. oryzae and Its Role in Virulence to Rice. Plant Pathol J. 36:289–
604 296.
605 Chow, J., and Mazmanian, S. K. 2010. A Pathobiont of the Microbiota Balances Host Colonization and
606 Intestinal Inflammation. Cell Host & Microbe. 7:265–276.
607 Cui, Z., Jin, G., Li, B., Kakar, K. U., Ojaghian, M. R., Wang, Y., et al. 2015. Gene Expression of Type VI
608 Secretion System Associated with Environmental Survival in Acidovorax avenae subsp. avenae by
609 Principle Component Analysis. Int J Mol Sci. 16:22008–22026.
610 Durand, E., Cambillau, C., Cascales, E., and Journet, L. 2014. VgrG, Tae, Tle, and beyond: the versatile
611 arsenal of Type VI secretion effectors. Trends in Microbiology. 22:498–507.
612 Durand, E., Nguyen, V. S., Zoued, A., Logger, L., Péhau-Arnaudet, G., Aschtgen, M.-S., et al. 2015.
613 Biogenesis and structure of a type VI secretion membrane core complex. Nature. 523:555–560.
614 Dutta, B., Gitaitis, R., Sanders, H., Booth, C., Smith, S., and Langston, D. B. 2014a. Role of blossom
615 colonization in pepper seed infestation by Xanthomonas euvesicatoria. Phytopathology. 104:232–
616 239.
617 Dutta, B., Gitaitis, R., Smith, S., and Langston, D. 2014b. Interactions of Seedborne Bacterial Pathogens
618 with Host and Non-Host Plants in Relation to Seed Infestation and Seedling Transmission. PLoS One.
619 9.
620 Freeman, B. C., Chen, C., Yu, X., Nielsen, L., Peterson, K., and Beattie, G. A. 2013. Physiological and
621 Transcriptional Responses to Osmotic Stress of Two Pseudomonas syringae Strains That Differ in
622 Epiphytic Fitness and Osmotolerance. J Bacteriol. 195:4742–4752.
623 Ge, Z., Sterzenbach, T., Whary, M., Rickman, B., Rogers, A., Shen, Z., et al. 2008. Helicobacter hepaticus
624 HHGI1 is a pathogenicity island associated with typhlocolitis in B6.129-IL10tm1Cgn mice. Microbes
625 Infect. 10:726–733.
626 Gitaitis, R., and Walcott, R. 2007. The Epidemiology and Management of Seedborne Bacterial Diseases.
627 Annu. Rev. Phytopathol. 45:371–397.
628 Helmann, T. C., Deutschbauer, A. M., and Lindow, S. E. 2019. Genome-wide identification of
629 *Pseudomonas syringae* genes required for fitness during colonization of the leaf surface and
630 apoplast. Proc Natl Acad Sci USA. 116:18900–18910.
631 Keen, N. T., Tamaki, S., Kobayashi, D., and Trollinger, D. 1988. Improved broad-host-range plasmids for
632 DNA cloning in Gram-negative bacteria. Gene. 70:191–197.
633 Kim, N., Kim, J. J., Kim, I., Mannaa, M., Park, J., Kim, J., et al. 2020. Type VI secretion systems of plant-
634 pathogenic Burkholderia glumae BGR1 play a functionally distinct role in interspecies interactions
635 and virulence. Molecular Plant Pathology. 21:1055–1069.
636 Lannou, C. 2012. Variation and selection of quantitative traits in plant pathogens. Annu Rev Phytopathol.
637 50:319–338.
638 Leung, K. Y., Siame, B. A., Snowball, H., and Mok, Y.-K. 2011. Type VI Secretion Regulation: Crosstalk and
639 Intracellular Communication. Current Opinion in Microbiology. 14 (1): 9–15.
640 Lindow, S., and Brandl, M.T. 2003. Microbiology of the phyllosphere. Appl. Environ. Microbiol. 69:1875-
641 1883.

642 Ma, L.-S., Hachani, A., Lin, J.-S., Filloux, A., and Lai, E.-M. 2014. Agrobacterium tumefaciens Deploys a
643 Superfamily of Type VI Secretion DNase Effectors as Weapons for Interbacterial Competition In
644 Planta. Cell Host & Microbe. 16:94–104.
645 Ma, L.-S., Narberhaus, F., and Lai, E.-M. 2012. IcmF family protein TssM exhibits ATPase activity and
646 energizes type VI secretion. J Biol Chem. 287:15610–15621.
647 MacIntyre, D. L., Miyata, S. T., Kitaoka, M., and Pukatzki, S. 2010. The Vibrio cholerae type VI secretion
648 system displays antimicrobial properties. Proc Natl Acad Sci U S A. 107:19520–19524.
649 Mattinen, L., Somervuo, P., Nykyri, J., Nissinen, R., Kouvonen, P., Corthals, G., et al. 2008. Microarray
650 profiling of host-extract-induced genes and characterization of the type VI secretion cluster in the
651 potato pathogen Pectobacterium atrosepticum. Microbiology. 154:2387–2396.
652 McAtee, P. A., Brian, L., Curran, B., van der Linden, O., Nieuwenhuizen, N. J., Chen, X., et al. 2018. Re-
653 programming of Pseudomonas syringae pv. actinidiae gene expression during early stages of
654 infection of kiwifruit. BMC Genomics. 19:822.
655 Meuskens, I., Saragliadis, A., Leo, J. C., and Linke, D. 2019. Type V Secretion Systems: An Overview of
656 Passenger Domain Functions. Front. Microbiol. 10:1163.
657 Miller, J. H. 1972. *Experiments in molecular genetics*. [Cold Spring Harbor, N.Y.]: Cold Spring Harbor
658 Laboratory.
659 Montenegro Benavides, N. A., Alvarez B., A., Arrieta-Ortiz, M. L., Rodriguez-R, L. M., Botero, D., Tabima,
660 J. F., et al. 2021. The type VI secretion system of Xanthomonas phaseoli pv. manihotis is involved in
661 virulence and in vitro motility. BMC Microbiology. 21:14.
662 Moscoso, J. A., Mikkelsen, H., Heeb, S., Williams, P., and Filloux, A. 2011. The Pseudomonas Aeruginosa
663 Sensor RetS Switches Type III and Type VI Secretion via C-Di-GMP Signalling. Environmental
664 Microbiology**.** 13 (12): 3128–3138.
665 Mougous, J. D. 2006. A Virulence Locus of Pseudomonas aeruginosa Encodes a Protein Secretion
666 Apparatus. Science. 312:1526–1530.
667 Navarro-Garcia, F., Ruiz-Perez, F., Cataldi, Á., and Larzábal, M. 2019. Type VI Secretion System in
668 Pathogenic Escherichia coli: Structure, Role in Virulence, and Acquisition. Front. Microbiol. 10
669 Newberry, E. A., Bhandari, R., Minsavage, G. V., Timilsina, S., Jibrin, M., Kemble, J., et al. 2019.
670 Independent evolution with the gene flux originating from multiple Xanthomonas species explains
671 genomic heterogeneity in Xanthomonas perforans. Appl. Environ. Microbiol. :AEM.00885-19.
672 de Pace, F., Boldrin de Paiva, J., Nakazato, G., Lancellotti, M., Sircili, M. P., Guedes Stehling, E., et al.
673 2011. Characterization of IcmF of the type VI secretion system in an avian pathogenic Escherichia
674 coli (APEC) strain. Microbiology. 157:2954–2962.
675 Palmer, T., Finney, A. J., Saha, C. K., Atkinson, G. C., and Sargent, F. 2020. A holin/peptidoglycan
676 hydrolase-dependent protein secretion system. Molecular Microbiology.
677 Pariaud, B., Robert, C., Goyeau, H., and Lannou, C. 2009. Aggressiveness components and adaptation to
678 a host cultivar in wheat leaf rust. Phytopathology. 99:869–878.
679 Parsons, D. A., and Heffron, F. 2005. sciS, an icmF Homolog in Salmonella enterica Serovar Typhimurium,
680 Limits Intracellular Replication and Decreases Virulence. Infect Immun. 73:4338–4345.
681 Pernezny, K., and Collins, J. 1997. Epiphytic Populations of Xanthomonas campestris pv. vesicatoria on
682 Pepper: Relationships to Host-Plant Resistance and Exposure to Copper Sprays. Plant Disease.
683 81:791–794.
684 Pezoa, D., Blondel, C. J., Silva, C. A., Yang, H.-J., Andrews-Polymenis, H., Santiviago, C. A., et al. 2014.
685 Only one of the two type VI secretion systems encoded in the Salmonella enterica serotype Dublin
686 genome is involved in colonization of the avian and murine hosts. Vet Res. 45:2.
687 Potnis, N., Timilsina, S., Strayer, A., Shantharaj, D., Barak, J. D., Paret, M. L., et al. 2015. Bacterial spot of
688 tomato and pepper: diverse Xanthomonas species with a wide variety of virulence factors posing a
689 worldwide challenge. Molecular Plant Pathology. 16:907–920.

690 Pukatzki, S., Ma, A. T., Sturtevant, D., Krastins, B., Sarracino, D., Nelson, W. C., et al. 2006. Identification
691 of a conserved bacterial protein secretion system in Vibrio cholerae using the Dictyostelium host
692 model system. Proceedings of the National Academy of Sciences. 103:1528–1533.
693 Records, A. R., and Gross, D. C. 2010. Sensor Kinases RetS and LadS Regulate Pseudomonas Syringae
694 Type VI Secretion and Virulence Factors. J Bacteriol. 192 (14): 3584–3596.
695 Russell, A. B., Hood, R. D., Bui, N. K., LeRoux, M., Vollmer, W., and Mougous, J. D. 2011. Type VI
696 secretion delivers bacteriolytic effectors to target cells. Nature. 475:343–347.
697 Sha, J., Rosenzweig, J. A., Kozlova, E. V., Wang, S., Erova, T. E., Kirtley, M. L., et al. 2013. Evaluation of the
698 roles played by Hcp and VgrG type 6 secretion system effectors in Aeromonas hydrophila SSU
699 pathogenesis. Microbiology (Reading). 159:1120–1135.
700 Shalom, G., Shaw, J. G., and Thomas, M. S. 2007. In vivo expression technology identifies a type VI
701 secretion system locus in Burkholderia pseudomallei that is induced upon invasion of macrophages.
702 Microbiology,. 153:2689–2699.
703 Song, L., Pan, J., Yang, Y., Zhang, Z., Cui, R., Jia, S., et al. 2021. Contact-independent killing mediated by a
704 T6SS effector with intrinsic cell-entry properties. Nature Communications. 12:423.
705 Storey, D., McNally, A., Åstrand, M., Santos, J. sa-P. G., Rodriguez-Escudero, I., Elmore, B., et al. 2020.
706 Klebsiella pneumoniae type VI secretion system-mediated microbial competition is PhoPQ
707 controlled and reactive oxygen species dependent. PLOS Pathogens. 16:e1007969.
708 Tian, Y., Zhao, Y., Shi, L., Cui, Z., Hu, B., and Zhao, Y. 2017. Type VI Secretion Systems of *Erwinia*
709 *amylovora* Contribute to Bacterial Competition, Virulence, and Exopolysaccharide Production.
710 Phytopathology. 107:654–661.
711 Tian, Y., Zhao, Y., Wu, X., Liu, F., Hu, B., and Walcott, R. R. 2015. The type VI protein secretion system
712 contributes to biofilm formation and seed-to-seedling transmission of *Acidovorax citrulli* on melon:
713 T6SS contributes to biofilm formation and seed-to-seedling transmission of *Acidovorax citrulli* on
714 melon. Molecular Plant Pathology. 16:38–47.
715 Trunk, K., Peltier, J., Liu, Y.-C., Dill, B. D., Walker, L., Gow, N. A. R., et al. 2018. The type VI secretion
716 system deploys antifungal effectors against microbial competitors. Nature Microbiology. 3:920–931.
717 Turner, P., Barber, C., and Daniels, M. 1984. Behaviour of the transposons Tn5 and Tn7 in Xanthomonas
718 campestris pv. campestris. Molecular and General Genetics MGG. 195:101–107.
719 Wang, N., Han, N., Tian, R., Chen, J., Gao, X., Wu, Z., et al. 2021. Role of the Type VI Secretion System in
720 the Pathogenicity of Pseudomonas syringae pv. actinidiae, the Causative Agent of Kiwifruit Bacterial
721 Canker. Frontiers in Microbiology. 12.
722 Weber, B. S., Miyata, S. T., Iwashkiw, J. A., Mortensen, B. L., Skaar, E. P., Pukatzki, S., et al. 2013.
723 Genomic and Functional Analysis of the Type VI Secretion System in Acinetobacter ed. Eric Cascales.
724 PLoS ONE. 8:e55142.
725 Wengelnik, K., Marie, C., Russel, M., and Bonas, U. 1996. Expression and localization of HrpA1, a protein
726 of Xanthomonas campestris pv. vesicatoria essential for pathogenicity and induction ofthe
727 hypersensitive reaction. J Bacteriol. 178:1061–1069.
728 Wu, H.-Y., Chung, P.-C., Shih, H.-W., Wen, S.-R., and Lai, E.-M. 2008. Secretome Analysis Uncovers an
729 Hcp-Family Protein Secreted via a Type VI Secretion System in Agrobacterium tumefaciens. J
730 Bacteriol. 190:2841–2850.
731 Zhang, L., Xu, J., Xu, J., Chen, K., He, L., and Feng, J. 2012. TssM is essential for virulence and required for
732 type VI secretion in Ralstonia solanacearum. J Plant Dis Prot. 119:125–134.
733 Zhang, W., Xu, S., Li, J., Shen, X., Wang, Y., and Yuan, Z. 2011. Modulation of a thermoregulated type VI
734 secretion system by AHL-dependent Quorum Sensing in Yersinia pseudotuberculosis. Arch
735 Microbiol. 193:351–363.

Zhu, P.-C., Li, Y.-M., Yang, X., Zou, H.-F., Zhu, X.-L., Niu, X.-N., et al. 2020. Type VI secretion system is not required for virulence on rice but for inter-bacterial competition in Xanthomonas oryzae pv. oryzicola. Res Microbiol. 171:64–73.

Zoued, A., Brunet, Y. R., Durand, E., Aschtgen, M.-S., Logger, L., Douzi, B., et al. 2014. Architecture and assembly of the Type VI secretion system. Biochimica et Biophysica Acta (BBA) - Molecular Cell Research. 1843:1664–1673.

Figure legends

Figure 1: Influence of mutation of *tssM* on disease symptom development. Figure shows disease symptoms by AL65, AL65*ΔtssM* or AL65*ΔtssM*(*tssM*) individual strains on the leaves of 4-5 week old tomato plants at 4 days after dip-inoculation. Water-soaked necrotic lesions were visible on leaves of the plants inoculated with the AL65*ΔtssM* as early as 3 days post-inoculation.

Figure 2: Effect of TssM on pathogenicity of *Xanthomonas perforans* AL65 using Dip inoculation assay. (a) Bacterial population growth upon individual strain inoculation (b) area under the growth progress curve calculated for each strain growth in individual inoculation (c) bacterial population growth in mixed inoculation AL65 + AL65*ΔtssM* , (d) area under the growth progress curve calculated for each strain growth in mixed inoculation AL65 + AL65*ΔtssM* (e) bacterial population growth mixed inoculation AL65*ΔtssM(tssM) +* AL65*ΔtssM,* (f) area under the growth progress curve calculated for each strain growth in mixed inoculation AL65*ΔtssM(tssM) +* AL65*ΔtssM* . 4-5-week-old Tomato (cv. FL8000) plants inoculated with ~1x 10^6 cfu/ml of AL65, AL65*ΔtssM* or AL65*ΔtssM*(*tssM*) individual strains or mixed inocula of AL65*ΔtssM(tssM) +* AL65*ΔtssM,* and AL65*ΔtssM(tssM) +* AL65*Δtss* were evaluated for bacterial population growth, every alternate day for 14 dpi on semi-selective media. Log_{10} cfu/cm^2 values were used to

761 calculate AUGPC values for each corresponding treatment. Lines represent the standard error of
762 the mean. A one-way ANOVA was applied for the statistical analysis of AUGPC and treatments
763 with different letters are significantly different according to Tukey's test of least significant
764 difference ($P<0.05$). A one-way ANOVA was applied for the statistical analysis of bacterial
765 population $\log_{10}$ values and treatments with * marks are significantly different according to
766 Tukey's test of least significant difference ($P<0.05$).

767 **Figure 3: Effect of TssM on symptom development of *Xanthomonas perforans* AL65-Dip**
768 **inoculation assay.** Disease severity index in individual inoculation (a) and in mixed inoculations
769 (b) on tomato leaves assessed every alternate day upto 14 days post-inoculation. (c) Symptom
770 development with AL65, AL65*ΔtssM* or AL65*ΔtssM*(*tssM*) was recorded at 14 days after
771 inoculation in case of individual strain inoculation and in mixed inoculations. 4-5-week-old
772 Tomato (cv. FL8000) plants inoculated with ~1x 10^6 cfu/ml of AL65, AL65*ΔtssM* or
773 AL65*ΔtssM*(*tssM*) strains were evaluated for disease development, every alternate day for 14
774 dpi. A one-way ANOVA was applied for the statistical analysis of disease index values on each
775 sampling day separately.

776 **Figure 4: Effect of TssM on pathogenicity of *Xanthomonas perforans* AL65 - Infiltration method**
777 (a) bacterial population growth on each sampling date (b) area under the growth progress curve
778 calculated for each strain (C) tomato leaves 8 days after inoculation with each strains . Four-to-
779 five-week-old Tomato cv. FL8000 plants were inoculated with cell suspensions containing ~1 X
780 10^5 cfu/ml of *X. perforans* AL65^{strep}/ AL65Δ*tssM*^{nal}/ AL65Δ*tssM*(*tssM*)^{km} using a needleless syringe
781 and were evaluated for bacterial population growth, every alternate day for 8 dpi on semi-

selective media. log_{10} cfu/cm^2 values were used to calculate AUGPC values for each corresponding treatment. A one-way ANOVA was applied for the statistical analysis of bacterial population log_{10} values and disease severity values on each sampling day separately and treatments with * marks are significantly different according to Tukey's test of least significant difference (P<0.05). A one-way ANOVA was applied for the statistical analysis of AUGPC and treatments with different letters are significantly different according to Tukey's test of least significant difference (P<0.05).

Figure 5: Impact of mutation of *tssM* on pathogen epiphytic colonization and dissemination under transplant-house mimic conditions. (a, b) Arrangement of the trays inside the humidity chambers and *X. perforans* survival under high-humidity conditions. First row of the two-week-old tomato seedlings in the 128 cell trays were inoculated with 1:1 ratio of either (a)AL65^{strep} and AL65*ΔtssM*^{nal} or (b)AL65*ΔtssM*^{nal} and AL65*ΔtssM*(*tssM*)^{km} and total and epiphytic populations were measured at each sampling point (S1-S9) at 7, 14, 21 and 28 dpi and used to calculate the AUGPC. (c, d) AUGPC using total population counts. Bars represent AUGPC values for total population of AL65^{strep} and AL65*ΔtssM*^{nal} when mixed inoculated in the first row S1 in chamber 1 (c), and AUGPC values for total population of AL65*ΔtssM*^{nal} and AL65*ΔtssM*(*tssM*) ^{km} when mixed inoculated in the first row S1 in chamber 2 (d). Figures e and f show AUGPC values calculated for epiphytic populations of WT, AL65*ΔtssM*^{nal} and AL65*ΔtssM*(*tssM*) ^{km} in chamber 1 and chamber 2. Vertical lines represent the standard error of the mean and General Linear Mixed models (GLMM) were applied to AUGPC values of each chamber for total and epiphytic populations separately using gradient as a variable. Different letters are significantly different according to the Tukey's test of least significant difference (P<0.05).

Figure 6: Effect of TssM on seed-to-seedling disease transmission of *Xanthomonas perforans* AL65 (A) bacterial population growth and (B) disease index in tomato (cv. FL8000) seedlings. Seeds were inoculated with ~1x 10^6 cfu/ml of AL65, AL65Δ*tssM* or AL65Δ*tssM*(*tssM*) strains and seedlings were evaluated 21 days after planting. Bars with standard deviation represent the means of two independent experiments. A one-way ANOVA was applied for the statistical analysis and treatments with different letters are significantly different according to the Tukey's test of least significant difference (P<0.05).

Figure 7: Role of TssM in osmotolerance. AL65, AL65 Δ*tssM* and AL65 Δ*tssM*(*tssM*) strains were grown in XVM2 media amended with different concentrations of NaCl, 0.02M, 0.1M and 0.2M. Optical density at 600nm was measured over time upto 60h after inoculation. Figures a, c and e show growth curve based on OD600 values in XVM2 medium amended with NaCl concentrations of 0.02M, 0.1M and 0.2M, respectively. In vitro bacterial population counts were taken at 0, 30 and 60h post-inoculation. Figures b, d, and f show in vitro population growth based on colony counts over time in XVM2 medium amended with NaCl concentrations of 0.02M, 0.1M and 0.2M, respectively. Vertical lines represent the standard error of the mean and General Linear Mixed models (GLMM) was performed for log cfu/ml values for each Nacl concentration separately using time as a variable. Different letters are significantly different according to the Tukey's test of least significant difference (P<0.05).

Figure S1: *X. perforans* survival under high-humidity conditions at 7days post inoculation. Total and epiphytic *X. perforans* population growth 7 days after inoculation of first row of the two-week- old tomato seedlings in the 128 cell trays with 1:1 ratio of either (a)$AL65^{strep}$ and

AL65*ΔtssM*^{nal} or (b)AL65*ΔtssM*^{nal} and AL65*ΔtssM*(*tssM*)^{km} and total and epiphytic populations were measured at each sampling point (S1-S9) (a) Bars represent the total population (cfu/g) values of chamber 1 where AL65^{strep} and AL65*ΔtssM*^{nal} were mixed inoculated and (d) bars represent the total population (cfu/g) values of chamber 2 where AL65*ΔtssM*^{nal} and AL65*ΔtssM*(*tssM*) ^{km} were mixed inoculated. (e) Line graph represent the epiphytic population (cfu/g) values of chamber 1 where AL65^{strep} and AL65*ΔtssM*^{na}were mixed inoculated. (f) line graph represent the epiphytic population (cfu/g) values of chamber 2 where AL65*ΔtssM*^{nal} and AL65*ΔtssM*(*tssM*) ^{km} were mixed inoculated. Vertical lines represent the standard error of the mean and General Linear Mixed models (GLMM) was performed for AUGPC values of each chamber for total and epiphytic populations separately using gradient as a variable. Different letters are significantly different according to the Tukey's test of least significant difference ($P<0.05$).

Figure S2: *X. perforans* survival under high-humidity conditions at 14 days post inoculation. Total and epiphytic *X. perforans* population growth 14 days after inoculation of first row of the two-week- old tomato seedlings in the 128 cell trays with 1:1 ratio of either (a)AL65^{strep} and AL65*ΔtssM*^{nal} or (b)AL65*ΔtssM*^{nal} and AL65*ΔtssM*(*tssM*)^{km} and total and epiphytic populations were measured at each sampling point (S1-S9) (a) Bars represent the total population (cfu/g) values of chamber 1 where AL65^{strep} and AL65*ΔtssM*^{nal} were mixed inoculated and (d) bars represent the total population (cfu/g) values of chamber 2 where AL65*ΔtssM*^{nal} and AL65*ΔtssM*(*tssM*) ^{km} were mixed inoculated. (e) Line graph represent the epiphytic population (cfu/g) values of chamber 1 where AL65^{strep} and AL65*ΔtssM*^{na}were mixed inoculated. (f) line graph represent the epiphytic population (cfu/g) values of chamber 2 where AL65*ΔtssM*^{nal} and

AL65*ΔtssM*(*tssM*) ^{km} were mixed inoculated. Vertical lines represent the standard error of the mean and General Linear Mixed models (GLMM) was performed for AUGPC values of each chamber for total and epiphytic populations separately using gradient as a variable. Different letters are significantly different according to the Tukey's test of least significant difference (P<0.05).

Figure S3: *X. perforans* survival under high-humidity conditions at 21 days post inoculation. Total and epiphytic *X. perforans* population growth 21 days after inoculation of first row of the two-week- old tomato seedlings in the 128 cell trays with 1:1 ratio of either (a)AL65^{strep} and AL65*ΔtssM*^{nal} or (b)AL65*ΔtssM*^{nal} and AL65*ΔtssM*(*tssM*)^{km} and total and epiphytic populations were measured at each sampling point (S1-S9) (a) Bars represent the total population (cfu/g) values of chamber 1 where AL65^{strep} and AL65*ΔtssM*^{nal} were mixed inoculated and (d) bars represent the total population (cfu/g) values of chamber 2 where AL65*ΔtssM*^{nal} and AL65*ΔtssM*(*tssM*) ^{km} were mixed inoculated. (e) Line graph represent the epiphytic population (cfu/g) values of chamber 1 where AL65^{strep} and AL65*ΔtssM*^{na}were mixed inoculated. (f) line graph represent the epiphytic population (cfu/g) values of chamber 2 where AL65*ΔtssM*^{nal} and AL65*ΔtssM*(*tssM*) ^{km} were mixed inoculated. Vertical lines represent the standard error of the mean and General Linear Mixed models (GLMM) was performed for AUGPC values of each chamber for total and epiphytic populations separately using gradient as a variable. Different letters are significantly different according to the Tukey's test of least significant difference (P<0.05).

Figure S4: *X. perforans* survival under high-humidity conditions at 28 days post inoculation. Total and epiphytic *X. perforans* population growth 28 days after inoculation of first row of the two-week- old tomato seedlings in the 128 cell trays with 1:1 ratio of either (a)AL65^{strep} and AL65*ΔtssM*^{nal} or (b)AL65*ΔtssM*^{nal} and AL65*ΔtssM*(*tssM*)^{km} and total and epiphytic populations were measured at each sampling point (S1-S9) (a) Bars represent the total population (cfu/g) values of chamber 1 where AL65^{strep} and AL65*ΔtssM*^{nal} were mixed inoculated and (d) bars represent the total population (cfu/g) values of chamber 2 where AL65*ΔtssM*^{nal} and AL65*ΔtssM*(*tssM*) ^{km} were mixed inoculated. (e) Line graph represent the epiphytic population (cfu/g) values of chamber 1 where AL65^{strep} and AL65*ΔtssM*^{na}were mixed inoculated. (f) line graph represent the epiphytic population (cfu/g) values of chamber 2 where AL65*ΔtssM*^{nal} and AL65*ΔtssM*(*tssM*) ^{km} were mixed inoculated. Vertical lines represent the standard error of the mean and General Linear Mixed models (GLMM) was performed for AUGPC values of each chamber for total and epiphytic populations separately using gradient as a variable. Different letters are significantly different according to the Tukey's test of least significant difference ($P<0.05$).

Figure S5: *X. perforans* disease symptom development under high-humidity conditions. Percentage of plants that showed disease symptoms (a) inside chamber 1 where AL65^{strep} and AL65*ΔtssM*^{nal} were mixed inoculated (b) inside chamber 2 where AL65*ΔtssM*^{nal} and AL65*ΔtssM(tssM)*^{km} were mixed inoculated. Surface plots were created to show the development of disease severity percentages of each sampling point during the course of the experiment.

889

890

891

892

893

894

895

896

897

898

899

900

901

902

903

904

905

906

907

908

909

910

911

912 Table 1. Bacterial strains and plasmids used in this study.

Strain or plasmid	Relevant characteristics	References or source
Xanthomonas perforans strains		
WT/ AL65	XpAL65, Rif^r, Strep^r	Laboratory collection (Newberry et al. 2019)
AL65Δ*tssM*	Strain *Xp*AL65, in-frame deletion in *tssM*, Nal^r	This study
AL65Δ*tssM*(*tssM*)	Strain *Xp*AL65, Δ*tssM* mutant complemented with pDSK519(*tssM*), Km^r	This study
Escherichia coli		
One Shot™ TOP10	F$^-$ *mcr*A Δ(*mrr-hsd*RMS-*mcr*BC) ϕ80*lac*ZΔM15Δ*lac*X74*rec*A1*ara*D139Δ(*ara-leu*) 7697 *gal*U *gal*K *rps*L (Str^r) *end*A1 *nup*G λ-	Invitrogen
DH5α	F− 80dlacZΔM15 Δ(lacZYA-argF)U169 endA1 deoR recA1 hsdR17(rK− mK+) phoA supE44 λ−thi-l gyrA96 relA1	Life Technologies, Carlsbad, CA
Plasmids		
pCR™8/GW/TOPO®	Topo cloning vector, Spec^r	Invitrogen
pCR™-Blunt II-TOPO®	Blunt DNA Cloning Vector, Km^r	Invitrogen
pLVC18-RfC	Tet^r, Gateway destination suicide vector	Roden et al. 2004
pLVC18-RfC (Δ*tssM*)	pLVC18 derivative containing fusion of genomic regions upstream and downstream of *tssM*, Tet^r	This study
pRK 2073	Helper plasmid	

pDSK519	Km^r	(Keen et al. 1988)
pDSK519 (*tssM*)	pDSK19 with genomic region containing coding region of *tssM* along with upstream and downstream flanking region of *tssM*; Km^r	This study

913 Rif^r, $Strep^r$, Km^r, Nal^r Nal^r, Str^r, $Spec^r$, Tet^r : ^{r} indicates antibiotic resistance respectively

Figure 1. Influence of mutation of *tssM* on disease symptom development. Figure shows disease symptoms by AL65, AL65Δ*tssM* or AL65Δ*tssM* (*tssM*) on the leaves of 4-5 week old tomato plants at 4 days post-inoculation. Water-soaked necrotic lesions were visible on leaves of plants inoculated with AL65Δ*tssM* as early as day 3 post-inoculation.

177x58mm (300 x 300 DPI)

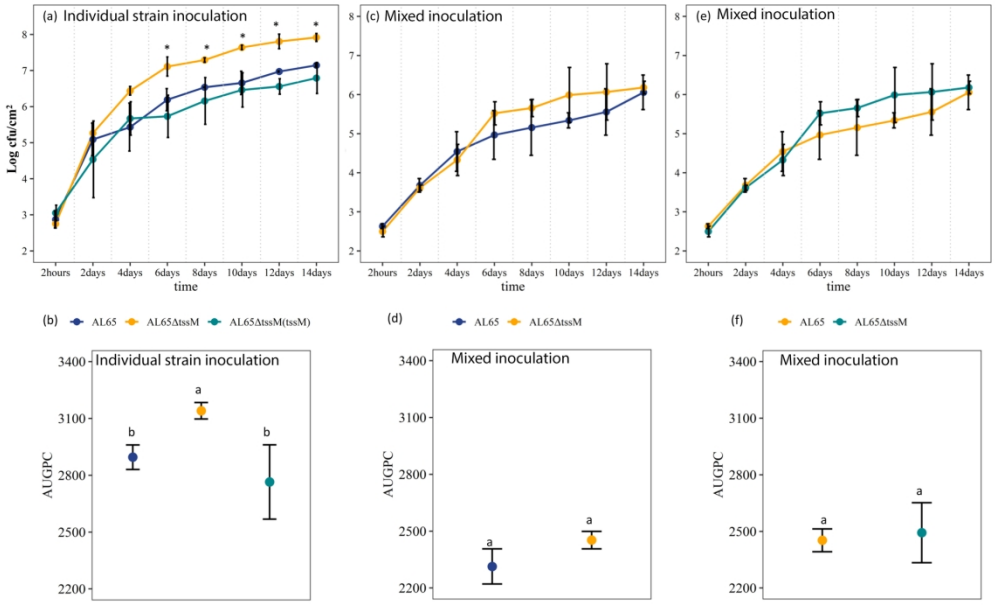

Figure 2: Effect of TssM on pathogenicity of *Xanthomonas perforans* AL65 using Dip inoculation assay. (a) Bacterial population growth upon individual strain inoculation (b) area under the growth progress curve calculated for each strain growth in individual inoculation (c) bacterial population growth in mixed inoculation AL65 + AL65*ΔtssM* , (d) area under the growth progress curve calculated for each strain growth in mixed inoculation AL65 + AL65*ΔtssM* (e) bacterial population growth mixed inoculation AL65*ΔtssM*(*tssM*) + AL65*ΔtssM*, (f) area under the growth progress curve calculated for each strain growth in mixed inoculation AL65*ΔtssM*(*tssM*) + AL65*ΔtssM*. 4-5-week-old Tomato (cv. FL8000) plants inoculated with ~1x 10^6 cfu/ml of AL65, AL65*ΔtssM* or AL65*ΔtssM*(*tssM*) individual strains or mixed inocula of AL65+AL65*ΔtssM*, and AL65*ΔtssM*+ AL65*ΔtssM*(*tssM*) were evaluated for bacterial population growth, every alternate day for 14 dpi on semi-selective media. Log_{10} cfu/cm^2 values were used to calculate AUGPC values for each corresponding treatment. Lines represent the standard error of the mean. A one-way ANOVA was applied for the statistical analysis of AUGPC and treatments with different letters are significantly different according to Tukey's test of least significant difference (P<0.05). A one-way ANOVA was applied for the statistical analysis of bacterial population log10 values and treatments with * marks are significantly different according to Tukey's test of least significant difference (P<0.05).

177x110mm (300 x 300 DPI)

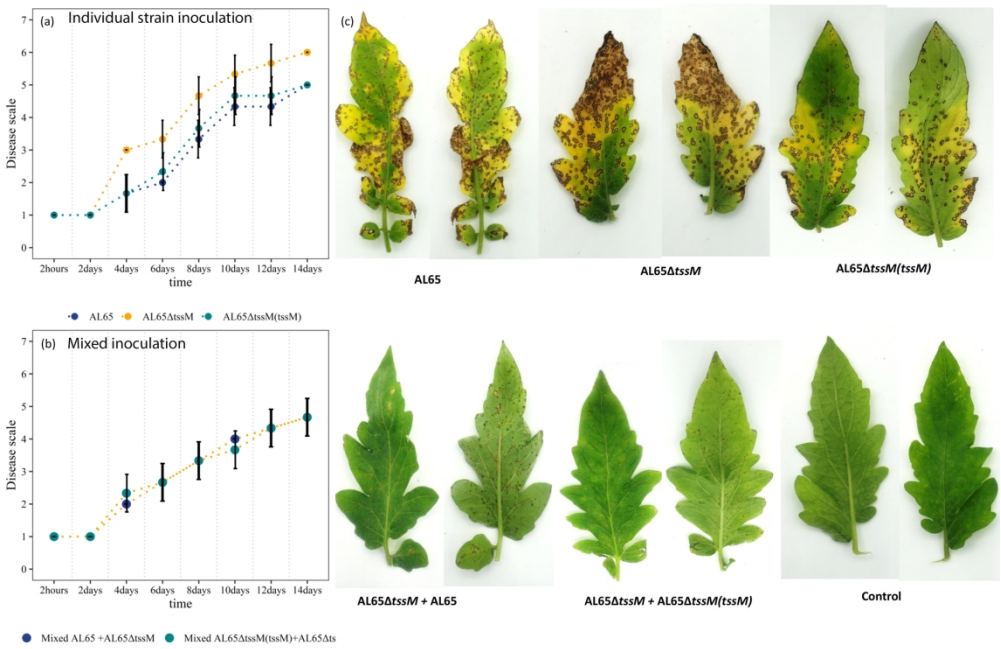

Figure 3: Effect of TssM on symptom development of *Xanthomonas perforans* AL65-Dip inoculation assay. Disease severity index in individual inoculation (a) and in mixed inoculations (b) on tomato leaves assessed every alternate day upto 14 days post-inoculation. (c) Symptom development with AL65, AL65Δ*tssM* or AL65Δ*tssM*(*tssM*) was recorded at 14 days after inoculation in case of individual strain inoculation and in mixed inoculations. 4-5-week-old Tomato (cv. FL8000) plants inoculated with ~1x 10^6 cfu/ml of AL65, AL65Δ*tssM* or AL65Δ*tssM*(*tssM*) strains were evaluated for disease development, every alternate day for 14 dpi. A one-way ANOVA was applied for the statistical analysis of disease index values on each sampling day separately.

177x116mm (300 x 300 DPI)

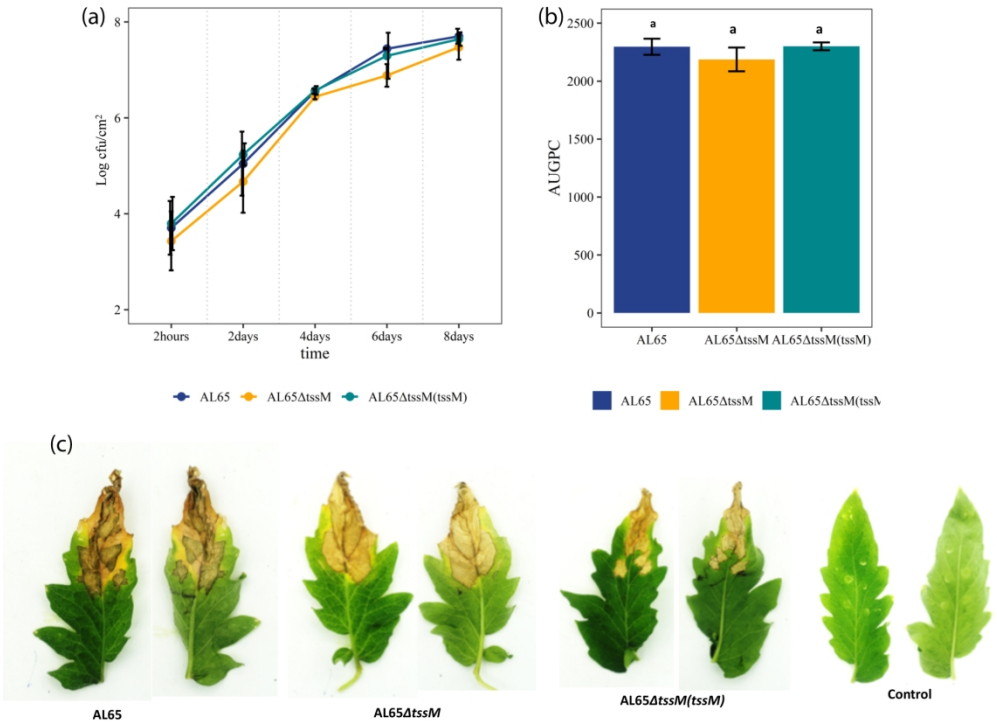

Figure 4: Effect of TssM on pathogenicity of *Xanthomonas perforans* AL65 - Infiltration method (a) bacterial population growth on each sampling date (b) area under the growth progress curve calculated for each strain (C) tomato leaves 8 days after infiltration with each strains . Four-to-five-week-old Tomato cv. FL8000 plants were infiltrated with cell suspensions containing ~1 X 10^5 cfu/ml of *X. perforans* AL65^{strep}, AL65*ΔtssM*^{nal} and, AL65*ΔtssM*(*tssM*) ^{Km} using a needleless syringe and were evaluated for bacterial population growth, every alternate day for 8 dpi on semi-selective media. log_{10} cfu/cm^2 values were used to calculate AUGPC values for each corresponding treatment. A one-way ANOVA was applied for the statistical analysis of bacterial population log10 values and disease severity values on each sampling day separately and treatments with * marks are significantly different according to Tukey's test of least significant difference (P<0.05). A one-way ANOVA was applied for the statistical analysis of AUGPC and treatments with different letters are significantly different according to Tukey's test of least significant difference (P<0.05).

177x133mm (300 x 300 DPI)

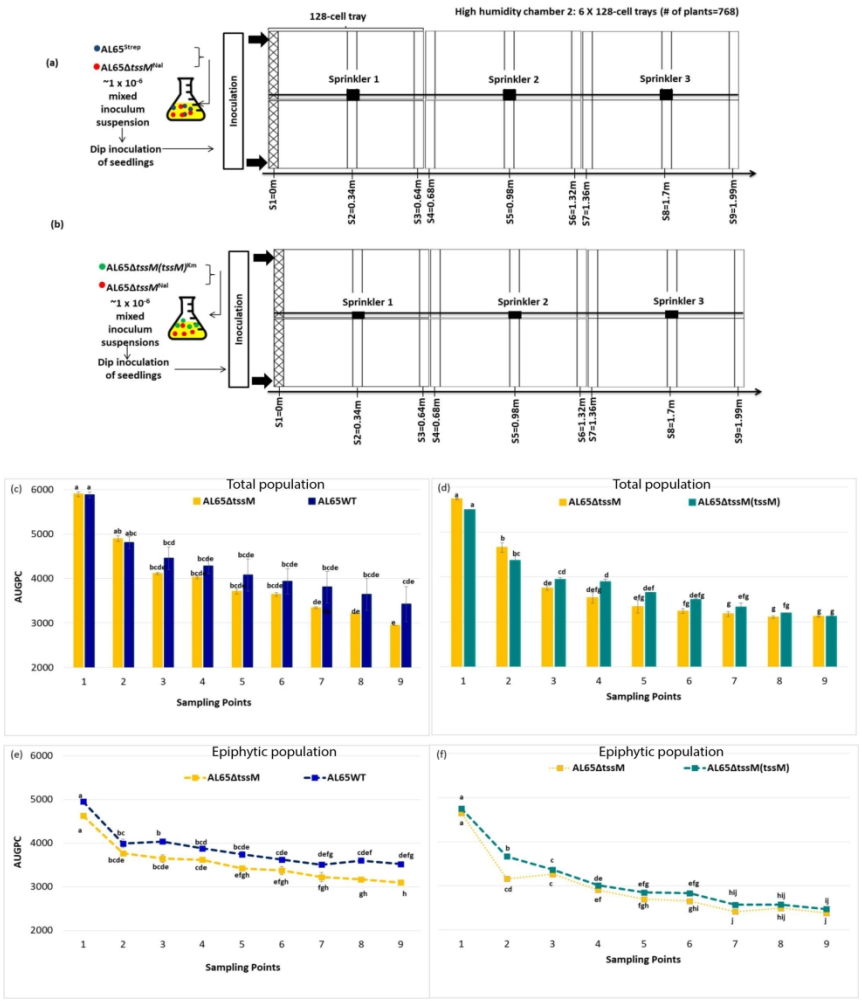

Figure 5: Impact of mutation of *tssM* on pathogen epiphytic colonization and dissemination under transplant-house mimic conditions. (a, b) Arrangement of the trays inside the humidity chambers and X. perforans survival under high-humidity conditions. First row of the two-week- old tomato seedlings in the 128 cell trays were inoculated with 1:1 ratio of either (a)AL65^{strep} and AL65*ΔtssM*^{Nal} or (b)AL65*ΔtssM*^{Nal} and AL65*ΔtssM*(*tssM*)^{Km} and total and epiphytic populations were measured at each sampling point (S1-S9) at 7, 14, 21 and 28 dpi and used to calculate the AUGPC. (c, d) AUGPC using total population counts. Bars represent AUGPC values for total population of AL65^{strep} and AL65*ΔtssM*^{Nal} when mixed inoculated in the first row S1 in chamber 1 (c), and AUGPC values for total population of AL65*ΔtssM*^{Nal} and AL65*ΔtssM*(*tssM*)^{Km} when mixed inoculated in the first row S1 in chamber 2 (d). Figures e and f show AUGPC values calculated for epiphytic populations of WT, AL65*ΔtssM*^{Nal} and AL65*ΔtssM*(*tssM*)^{Km} in chamber 1 and chamber 2. Vertical lines represent the standard error of the mean and General Linear Mixed models (GLMM) were applied to AUGPC values of each chamber for total and epiphytic populations separately using

gradient as a variable. Different letters are significantly different according to the Tukey’s test of least significant difference (P<0.05).

177x245mm (300 x 300 DPI)

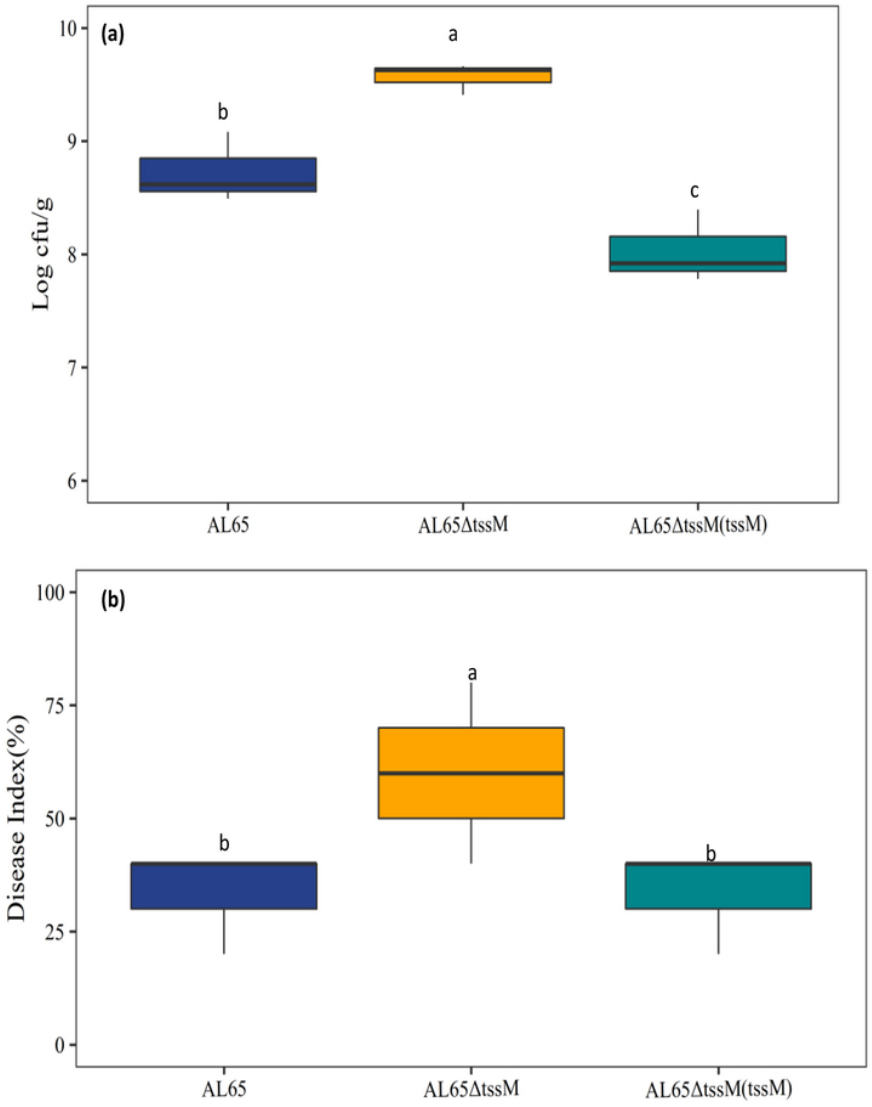

Figure 6: Effect of TssM on seed-to-seedling disease transmission of *Xanthomonas perforans* AL65 (A) bacterial population growth and (B) disease index in tomato (cv. FL8000) seedlings. Seeds were inoculated with ~1x 10^6 cfu/ml of AL65, AL65*ΔtssM* or AL65*ΔtssM*(*tssM*) strains and seedlings were evaluated 21 days after planting. Bars with standard deviation represent the means of two independent experiments. A one-way ANOVA was applied for the statistical analysis and treatments with different letters are significantly different according to the Tukey's test of least significant difference ($P<0.05$).

67x83mm (300 x 300 DPI)

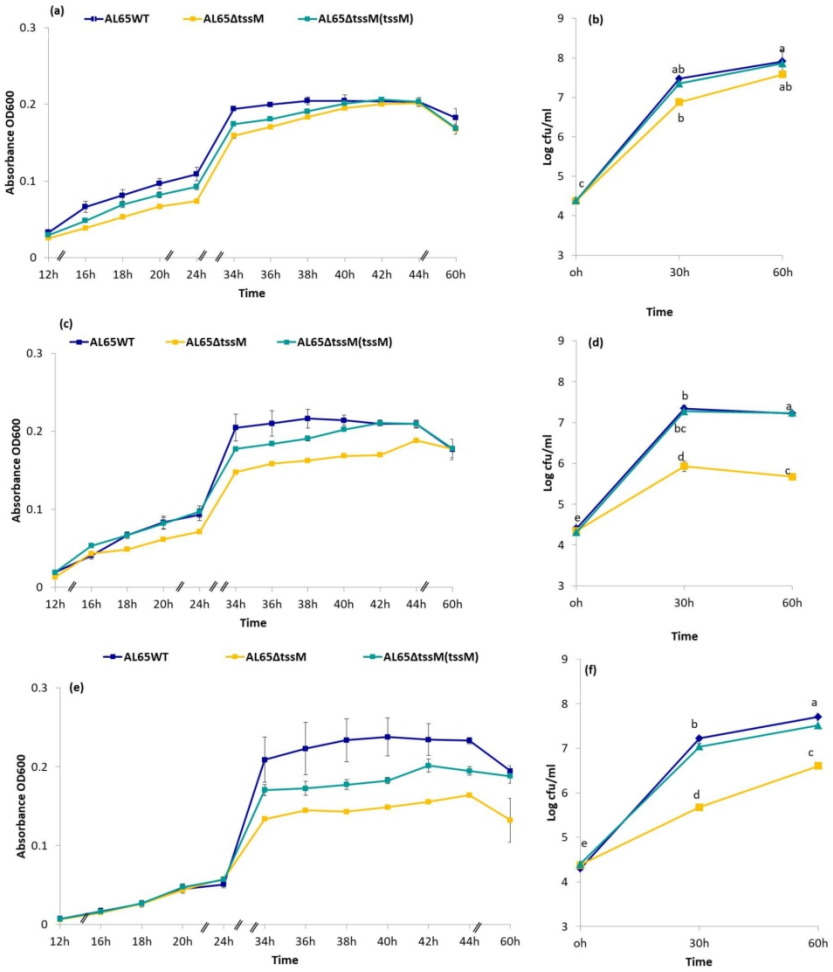

Figure 7: Role of TssM in osmotolerance. AL65, AL65*ΔtssM* and AL65*ΔtssM*(*tssM*) strains were grown in XVM2 media amended with different concentrations of NaCl, 0.02M, 0.1M and 0.2M. Optical density at 600nm was measured over time upto 60h after inoculation. Figures a, c and e show growth curve based on OD_{600} values in XVM2 medium amended with NaCl concentrations of 0.02M, 0.1M and 0.2M, respectively. In vitro bacterial population counts were taken at 0, 30 and 60h post-inoculation. Figures b, d, and f show in vitro population growth based on colony counts over time in XVM2 medium amended with NaCl concentrations of 0.02M, 0.1M and 0.2M, respectively. Vertical lines represent the standard error of the mean and General Linear Mixed models (GLMM) was performed for log cfu/ml values for each NaCl concentration separately using time as a variable. Different letters are significantly different according to the Tukey's test of least significant difference ($P<0.05$).

177x177mm (300 x 300 DPI)

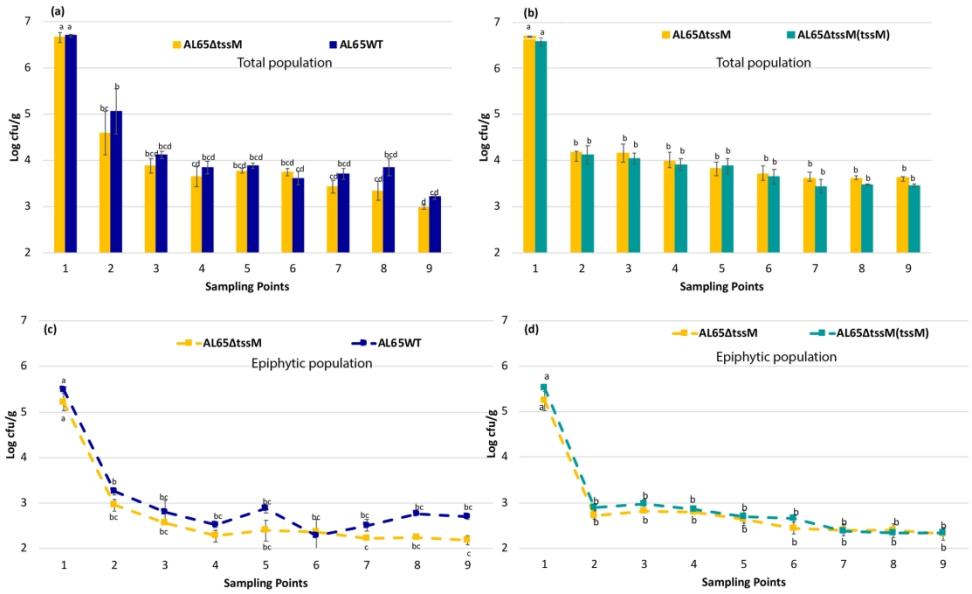

Figure S1: *X. perforans* survival under high-humidity conditions at 7 days post inoculation. Total and epiphytic *X. perforans* population growth 7 days after inoculation of first row of the two-week- old tomato seedlings in the 128 cell trays with 1:1 ratio of either (a)AL65^{strep} and AL65*ΔtssM*^{nal} or (b)AL65*ΔtssM*^{nal} and AL65*ΔtssM*(*tssM*)^{km} and total and epiphytic populations were measured at each sampling point (S1-S9) (a) Bars represent the total population (cfu/g) values of chamber 1 where AL65^{strep} and AL65*ΔtssM*^{nal} were mixed inoculated and (d) bars represent the total population (cfu/g) values of chamber 2 where AL65*ΔtssM*^{nal} and AL65*ΔtssM*(*tssM*)^{km} were mixed inoculated. (e) Line graph represent the epiphytic population (cfu/g) values of chamber 1 where AL65^{strep} and AL65*ΔtssM*^{nal} were mixed inoculated. (f) line graph represent the epiphytic population (cfu/g) values of chamber 2 where AL65*ΔtssM*^{nal} and AL65*ΔtssM*(*tssM*)^{km} were mixed inoculated. Vertical lines represent the standard error of the mean and General Linear Mixed models (GLMM) was performed for AUGPC values of each chamber for total and epiphytic populations separately using gradient as a variable. Different letters are significantly different according to the Tukey's test of least significant difference ($P<0.05$).

177x112mm (300 x 300 DPI)

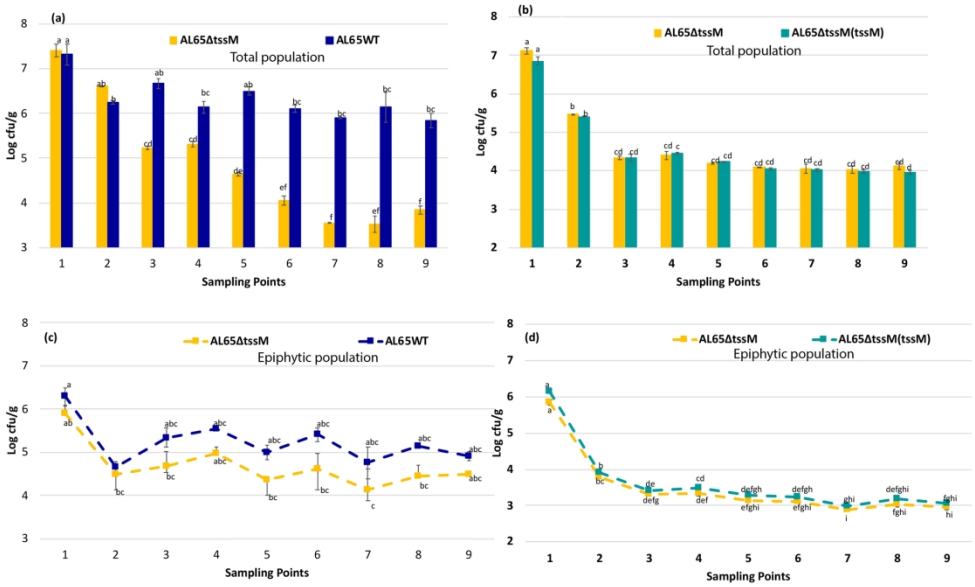

Figure S2: *X. perforans* survival under high-humidity conditions at 14 days post inoculation. Total and epiphytic *X. perforans* population growth 14 days after inoculation of first row of the two-week- old tomato seedlings in the 128 cell trays with 1:1 ratio of either (a)AL65^{strep} and AL65*ΔtssM*^{nal} or (b)AL65*ΔtssM*^{nal} and AL65*ΔtssM*(*tssM*)^{km} and total and epiphytic populations were measured at each sampling point (S1-S9) (a) Bars represent the total population (cfu/g) values of chamber 1 where AL65^{strep} and AL65*ΔtssM*^{nal} were mixed inoculated and (d) bars represent the total population (cfu/g) values of chamber 2 where AL65*ΔtssM*^{nal} and AL65*ΔtssM*(*tssM*)^{km} were mixed inoculated. (e) Line graph represent the epiphytic population (cfu/g) values of chamber 1 where AL65^{strep} and AL65*ΔtssM*^{nal} were mixed inoculated. (f) line graph represent the epiphytic population (cfu/g) values of chamber 2 where AL65*ΔtssM*^{nal} and AL65*ΔtssM*(*tssM*)^{km} were mixed inoculated. Vertical lines represent the standard error of the mean and General Linear Mixed models (GLMM) was performed for AUGPC values of each chamber for total and epiphytic populations separately using gradient as a variable. Different letters are significantly different according to the Tukey's test of least significant difference ($P<0.05$).

177x107mm (300 x 300 DPI)

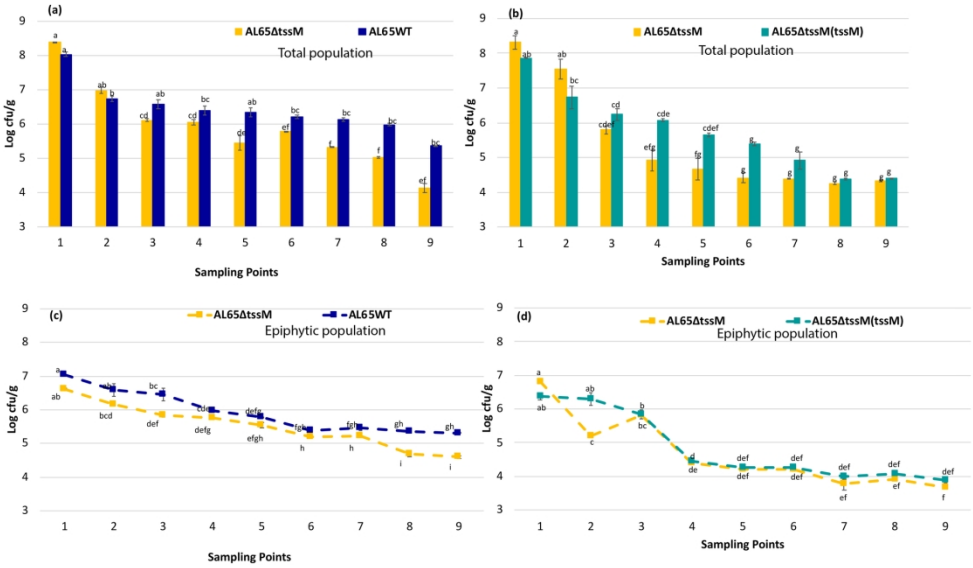

Figure S3: *X. perforans* survival under high-humidity conditions at 21 days post inoculation. Total and epiphytic *X. perforans* population growth 21 days after inoculation of first row of the two-week- old tomato seedlings in the 128 cell trays with 1:1 ratio of either (a)AL65^{strep} and AL65*ΔtssM*^{nal} or (b)AL65*ΔtssM*^{nal} and AL65*ΔtssM*(*tssM*)^{km} and total and epiphytic populations were measured at each sampling point (S1-S9) (a) Bars represent the total population (cfu/g) values of chamber 1 where AL65^{strep} and AL65*ΔtssM*^{nal} were mixed inoculated and (d) bars represent the total population (cfu/g) values of chamber 2 where AL65*ΔtssM*^{nal} and AL65*ΔtssM*(*tssM*)^{km} were mixed inoculated. (e) Line graph represent the epiphytic population (cfu/g) values of chamber 1 where AL65^{strep} and AL65*ΔtssM*^{nal} were mixed inoculated. (f) line graph represent the epiphytic population (cfu/g) values of chamber 2 where AL65*ΔtssM*^{nal} and AL65*ΔtssM*(*tssM*)^{km} were mixed inoculated. Vertical lines represent the standard error of the mean and General Linear Mixed models (GLMM) was performed for AUGPC values of each chamber for total and epiphytic populations separately using gradient as a variable. Different letters are significantly different according to the Tukey's test of least significant difference ($P<0.05$).

177x104mm (300 x 300 DPI)

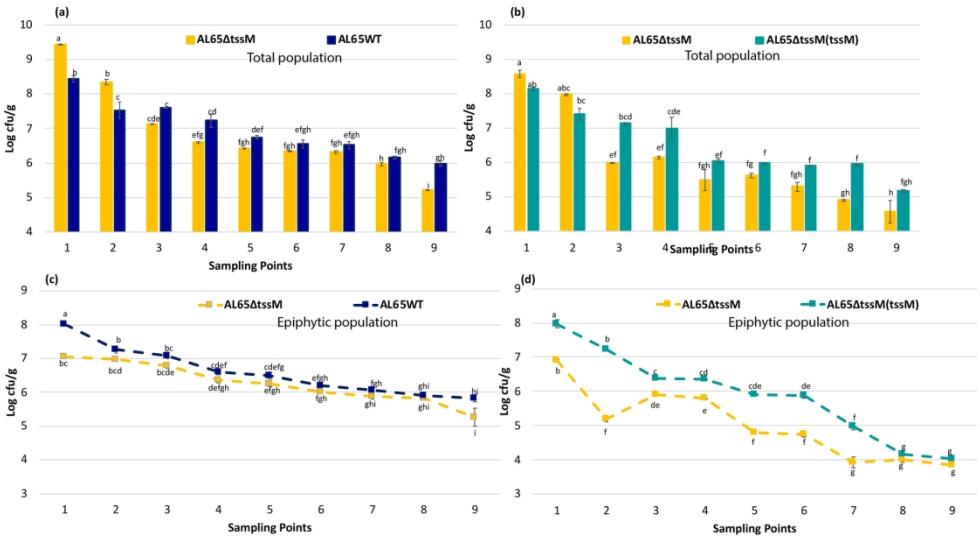

Figure S4: *X. perforans* survival under high-humidity conditions at 28 days post inoculation. Total and epiphytic *X. perforans* population growth 28 days after inoculation of first row of the two-week- old tomato seedlings in the 128 cell trays with 1:1 ratio of either (a)AL65^{strep} and AL65*ΔtssM*^{nal} or (b)AL65*ΔtssM*^{nal} and AL65*ΔtssM*(*tssM*)^{km} and total and epiphytic populations were measured at each sampling point (S1-S9) (a) Bars represent the total population (cfu/g) values of chamber 1 where AL65^{strep} and AL65*ΔtssM*^{nal} were mixed inoculated and (d) bars represent the total population (cfu/g) values of chamber 2 where AL65*ΔtssM*^{nal} and AL65*ΔtssM*(*tssM*)^{km} were mixed inoculated. (e) Line graph represent the epiphytic population (cfu/g) values of chamber 1 where AL65^{strep} and AL65*ΔtssM*^{nal} were mixed inoculated. (f) line graph represent the epiphytic population (cfu/g) values of chamber 2 where AL65*ΔtssM*^{nal} and AL65*ΔtssM*(*tssM*)^{km} were mixed inoculated. Vertical lines represent the standard error of the mean and General Linear Mixed models (GLMM) was performed for AUGPC values of each chamber for total and epiphytic populations separately using gradient as a variable. Different letters are significantly different according to the Tukey's test of least significant difference ($P<0.05$).

177x100mm (300 x 300 DPI)

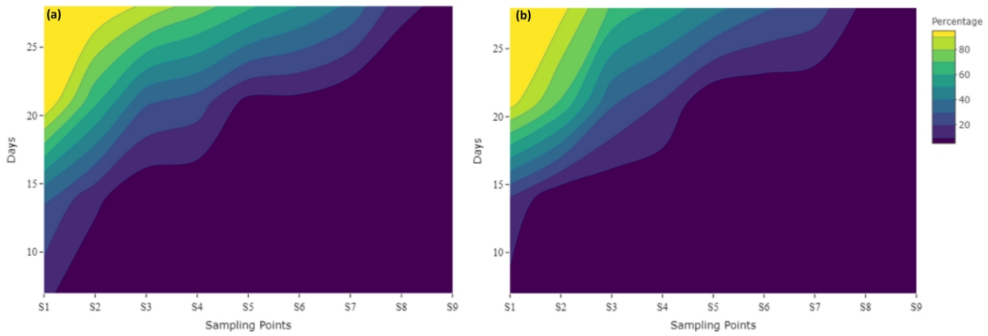

Figure S5: *X. perforans* disease symptom development under high-humidity conditions. Percentage of plants that showed disease symptoms (a) inside chamber 1 where AL65^{strep} and AL65Δ*tssM*^{nal} were mixed inoculated (b) inside chamber 2 where AL65Δ*tssM*^{nal} and AL65Δ*tssM*(*tssM*)^{km} were mixed inoculated. Surface plots were created to show the development of disease severity percentages of each sampling point during the course of the experiment

177x64mm (300 x 300 DPI)